



HAL
open science

A search for Low Surface Brightness galaxies in the near-infrared. II. Arecibo H I line observations

Delphine Monnier-Ragaine, Willem van Driel, K. O'Neil, S. E. Schneider,
Chantal Balkowski, Thomas H. Jarrett

► To cite this version:

Delphine Monnier-Ragaine, Willem van Driel, K. O'Neil, S. E. Schneider, Chantal Balkowski, et al..
A search for Low Surface Brightness galaxies in the near-infrared. II. Arecibo H I line observations.
Astronomy & Astrophysics - A&A, 2003, 408, pp.67-78. 10.1051/0004-6361:20030694 . hal-03785524

HAL Id: hal-03785524

<https://hal.science/hal-03785524v1>

Submitted on 25 Sep 2022

HAL is a multi-disciplinary open access archive for the deposit and dissemination of scientific research documents, whether they are published or not. The documents may come from teaching and research institutions in France or abroad, or from public or private research centers.

L'archive ouverte pluridisciplinaire **HAL**, est destinée au dépôt et à la diffusion de documents scientifiques de niveau recherche, publiés ou non, émanant des établissements d'enseignement et de recherche français ou étrangers, des laboratoires publics ou privés.

A search for Low Surface Brightness galaxies in the near-infrared

II. Arecibo H I line observations^{*}

D. Monnier Ragaigne¹, W. van Driel¹, K. O’Neil², S. E. Schneider³, C. Balkowski¹, and T. H. Jarrett⁴

¹ Observatoire de Paris, GEPI, CNRS UMR 8111 and Université Paris 7, 5 place Jules Janssen, 92195 Meudon Cedex, France
e-mail: delphine.ragaigne@obspm.fr; wim.vandriel@obspm.fr; chantal.balkowski@obspm.fr

² NRAO, PO Box 2, Green Bank, WV 24944, USA
e-mail: koneil@nrao.edu

³ University of Massachusetts, Astronomy Program, 536 LGRC, Amherst, MA 01003, USA
e-mail: schneide@messier.astro.umass.edu

⁴ IPAC, Caltech, MS 100-22, 770 South Wilson Ave., Pasadena, CA 91125, USA
e-mail: jarrett@ipac.caltech.edu

Received 19 February 2003 / Accepted 28 April 2003

Abstract. A total of 367 Low Surface Brightness galaxies detected in the 2MASS all-sky near-infrared survey have been observed in the 21 cm HI line using the Arecibo telescope. All have a K_s -band mean central surface brightness, measured within a $5''$ radius, fainter than $18 \text{ mag arcsec}^{-2}$. We present global HI line parameters for the 107 clearly detected objects and the 21 marginal detections, as well as upper limits for the undetected objects. The 107 clear detections comprise 15 previously uncatalogued objects and 36 with a PGC entry only.

Key words. galaxies: distances and redshifts – galaxies: general – galaxies: ISM – infrared: galaxies – radio lines: galaxies

1. Introduction

The present paper is part of a series presenting the results of a multi-wavelength (near-infrared, 21-cm HI line and optical) search for Low Surface Brightness (LSB) galaxies using the 2MASS all-sky near-infrared survey. For further details on the sample and other publications in this series, we refer to Monnier Ragaigne et al. (2003a, Paper I).

1.1. Low surface brightness galaxies

Observational bias in the selection of galaxies dates back to Messier and Herschel. Galaxies are diffuse objects selected in the presence of a contaminating signal: the brightness of the night sky. The night sky acts as a filter, which, when convolved with the true population of galaxies gives the population of galaxies we observe. In the past few decades, observations of the local universe have shown the existence of galaxies well below the surface brightness of the average catalogued galaxy.

At present, the LSBs constitute the least well known fraction of galaxies: their number density and physical properties (luminosity, colours, dynamics) are still quite uncertain.

Send offprint requests to: W. van Driel,
e-mail: win.vandriel@obspm.fr

^{*} Tables 2, 4a, 4b, 5a, 5b and Figs. 2, 3 are only available in electronic form at <http://www.edpsciences.org>

This is, by definition, mainly due to the fundamental difficulty in identifying them in imaging surveys and in measuring their properties. In order to further investigate the often baffling properties of the LSB class of galaxies we selected a sample of them from the 2MASS database, accessing a wavelength domain (the near-infrared) hitherto only scarcely explored in the study of LSBs.

There is no unambiguous definition of LSB galaxies, although ones in common use are based on (1) the mean blue surface brightness within the $25 \text{ mag arcsec}^{-2}$ isophote, (2) the mean surface brightness within the half-light radius, or (3) the extrapolated central surface brightness of the disc component alone after carrying out a disc-bulge decomposition. For 2MASS galaxies, we used the mean K_s -band magnitude within a fixed aperture to identify a sample of galaxies with relatively low infrared surface brightness. Because galaxies typically have $(B - K) \sim 3.5\text{--}4$ (see below) we selected galaxies in which the central surface brightness within a $5''$ radius circular aperture was fainter than $18 \text{ mag arcsec}^{-2}$ in K_s . This criterion corresponds roughly to the disc-component definition of LSB galaxies which have a blue central surface brightness $\mu_{B_0} > 22.0 \text{ mag arcsec}^{-2}$. Our sample galaxies can have even lower disc surface brightness levels if the bulge component is significant, but since we average over a fixed angular aperture, we may also include some higher central surface brightness sources that are more distant so that the aperture

includes more of the disc. In this paper, we examine the properties of our sample based on 2MASS and HyperLeda data and compare it to optically-selected galaxy samples.

LSBs have remarkable properties which distinguish them from high surface brightness spirals, notably:

- LSBs seem to constitute at least 50% of the total galaxy population in number in the local Universe, which may have strong implications for the slope of the galaxy luminosity function, on the baryonic matter density and especially on galaxy formation scenarios (O’Neil & Bothun 2000);
- LSBs discs are among the less evolved objects in the local universe since they have a very low star formation rate (van der Hulst et al. 1993; van Zee et al. 1997; van den Hoek et al. 2000);
- LSBs are embedded in dark matter halos which are of lower density and more extended than the haloes around High Surface Brightness (HSB) galaxies, and they are strongly dominated by Dark Matter at all radii (de Blok et al. 1996; McGaugh et al. 2001).

The star formation history of LSBs has been the subject of recent debate. The LSBs best studied in the optical and in the near-infrared are blue (e.g., Bergvall et al. 1999), indicating a young mean stellar age and/or metallicity. Morphologically, most studied LSBs have discs, but little spiral structure. The current massive star formation rates in LSBs are an order of magnitude lower than those of HSBs (van Zee et al. 1997); HI observations show that LSBs have high gas mass fractions, sometimes exceeding unity (Spitzak & Schneider 1998; McGaugh & de Blok 1997). All these observations are consistent with a scenario in which LSBs are relatively unevolved, low mass surface density, low metallicity systems with roughly constant star formation rate. However, this scenario has difficulty accomodating giant LSBs like Malin 1 (Bothun et al. 1987).

This study of infrared LSBs was also intended to investigate the possibility of there being a substantial population of red LSBs like those reported by O’Neil et al. (1997). Follow-up studies initially indicated that these red LSBs had rapid rotational speeds exceeding 200 km s^{-1} and they did not seem to follow the “standard” Tully-Fisher relation, in the sense that they appeared to be severely underluminous for their total mass (O’Neil et al. 2000). More recent observations by Chung et al. (2002) indicate that the rotational properties of these red LSBs were mismeasured due to confusion with neighbouring galaxies. An infrared-selected sample should allow us to identify whether there is a significant population of very red LSBs.

In the present paper a result of 21-cm HI line observations made at Arecibo is given, while in Paper I in the series a description of the 2MASS LSB galaxy sample selection is given, 21-cm HI line observations from Nançay will be presented in Paper III (Monnier Ragaigine et al. 2003b), optical *BVRI* CCD surface photometry of a sub-sample of 35 2MASS LSB galaxies will be presented in Paper IV (Monnier Ragaigine et al. 2003c), models of the star formation history of these, and an analysis of the full data set will be presented in Paper V.

Models of the evolution of the 2MASS galaxies presented in Paper IV and of other samples of LSB galaxies are presented in Boissier et al. (2003).

The 2MASS LSB galaxies sample selection is described in Sect. 2. Observations and data reduction are presented in Sect. 3, and the results in Sect. 4 and the conclusions in Sect. 5.

1.2. The 2MASS all-sky near-infrared survey

The Two Micron All Sky Survey, 2MASS, has imaged the entire celestial sphere in the near-infrared *J* ($1.25 \mu\text{m}$), *H* ($1.65 \mu\text{m}$) and *K_s* ($2.16 \mu\text{m}$) bands from two dedicated, identical 1.3-meter telescopes. The 2MASS data have a 95% completeness level in *J*, *H* and *K_s* of 15.1, 14.3 and 13.5 mag, respectively, for “normal” galaxies (Jarrett et al. 2000a); for LSB and blue objects the completeness limits are not yet known). The Extended Source Catalog (XSC) will consist of more than 1.4 million galaxies brighter than 14th mag at *K_s* with angular diameters greater than ~ 6 arcsec. The photometry includes accurate PSF-derived measures and a variety of circular and elliptical aperture measures, fully characterizing both point-like and extended objects. The position centroids have an astrometric accuracy better than ~ 0.5 arcsec. In addition to tabular information, 2MASS archives full-resolution images for each extended object, enabling detailed comparison with other imaging surveys. Initial results for galaxies detected by 2MASS are described in several publications (Schneider et al. 1997; Jarrett et al. 2000a, 2000b; Hurt et al. 2000).

Although relatively less deep than some of the dedicated optical imaging surveys made of LSB galaxies over limited areas of the sky, the 2MASS survey allows the detection of LSB galaxies with a central surface brightness in the *K_s* band of $\sim 18\text{--}20 \text{ mag arcsec}^{-2}$, corresponding to about $\sim 22\text{--}24 \text{ mag arcsec}^{-2}$ in *B*, extending over the entire sky. The near-infrared data will be less susceptible than optical surveys to the effects of extinction due to dust, both Galactic and internal to the galaxies.

In the present paper the HI line observations made at Arecibo of the sample of 2MASS near-infrared selected LSB galaxies is presented. The sample selection is described in Sect. 2. The observations and the data reduction are presented in Sect. 3, and the results in Sect. 4. A brief discussion of the results is given in Sect. 5. An analysis of these observations, and of others made for the study, will be given in a future paper (Paper V).

2. Sample selection

We have selected 2MASS LSB galaxies using the following two galaxy search routines. For a more complete description of the selection procedures we refer to Paper I. The selected LSB objects lie outside the ZoA ($|b| > 10^\circ$), but we have also observed 116 objects within this zone (see Sect. 4.6).

- The first is aimed at selecting relatively high signal-to-noise low central surface brightness (LCSB) galaxies, with a mean central *K_s* surface brightness in the inner $5''$ radius of $K_5 \geq 18 \text{ mag arcsec}^{-2}$, among the extended sources picked

out from the survey data by the standard 2MASS algorithms (Jarrett et al. 2000).

- The second is aimed at finding lower signal-to-noise LSB galaxies among those sources which were not recognized as such during the standard extended source selection described above. This requires masking all sources detected by the former method, spatially smoothing the remaining data and running the extended source recognition scheme again on the masked images.

In order to decide which of these faint, fuzzy 2MASS sources really are LSB galaxies, additional data were required like those listed in online databases such as NED (NASA Extragalactic Database) (<http://nedwww.ipac.caltech.edu>), LEDA (Lyon-Meudon Extragalactic Database) – recently incorporated in HyperLeda (<http://www-obs.univ-lyon1.fr/hypercat/>) – and Aladin of the Centre de Données astronomiques de Strasbourg (CDS) (<http://aladin.u-strasbg.fr>) and by inspecting Digital Sky Survey (DSS) images. Using this selection procedure, a total of 3800 candidate 2MASS LSB galaxies were found.

The source selection for our survey was made with the 2MASS working database available in late 1999, when work on it was still in full progress. The sources we observed at Arecibo contain only 2 “Small” sources (with isophotal radii $10'' < r_{K20} < 20''$, see Sect. 4.1), S721N and S1090O, that are not found in the subsequent, more reliable, 2MASS public data releases (see Paper I for details). Their names have been put in parentheses in the Tables. The sample also contains 2 Faint sources (F1N and F10N) that are not found in subsequent public data releases, which not surprising considering they were detected by a dedicated LSB galaxy search method and that they were not included in the working database.

Due to constraints in the telescope time scheduling and in the declination range accessible with the instrument, the area of the sky observed at Arecibo for our survey ranges from $20^{\text{h}}00^{\text{m}}$ to $06^{\text{h}}30^{\text{m}}$ in right ascension and between 12° and 39° in declination. Within this area, we selected for observation, in order of decreasing priority: (1) all objects with known velocity, (2) objects without known velocity, whether previously catalogued or not, in order of decreasing diameter.

3. Observations and data reduction

3.1. Observations

We observed a sample (see Sect. 2) of 367 2MASS LSB galaxies using the refurbished 305-m Arecibo Gregorian radio telescope in November 2000 and January 2001, for a total of 125 hours observing time. Data were taken with the *L*-band narrow receiver using nine-level sampling with two of the 2048 lag subcorrelators set to each polarization channel. All observations were taken using the position-switching technique, with the blank sky (or OFF) observation taken for the same length of time, and over the same portion of the Arecibo dish (as defined by the azimuth and zenith angles) as was used for the on-source (ON) observation. Each ON+OFF pair was followed by a 10 s ON+OFF observation of a well calibrated, uncorrelated noise diode. The observing strategy used was as

follows: first, a minimum of one 3 min ON/OFF pair was taken of each galaxy, followed by a 10 s ON/OFF calibration pair. If a galaxy was not detected, one or more additional 3 min ON/OFF pairs were taken of the object, if it was deemed of sufficient interest (e.g., large diameter, known optical velocity). If a galaxy’s velocity was known a priori, it was observed with each of the four 12.5 MHz bandpass subcorrelators being centred at the redshifted HI line of the galaxy. All galaxies without known velocities were observed in velocity search mode. In this mode the subcorrelators were set to 25 MHz bandpasses. Both subcorrelators with the same polarization were set to overlap by only 5 MHz, thereby allowing a wide velocity search while ensuring the overlapping region of the two boards was adequately covered. Two different velocity searches were made – first in the velocity range -500 to $11\,000$ km s^{-1} and subsequently in the range 9500 to $21\,000$ km s^{-1} (assuming the galaxy was not detected in the lower velocity range, the interest of the particular object and observing time permitting). The instrument’s HPBW at 21 cm is $3'.6 \times 3'.6$ and the pointing accuracy is about $15''$.

3.2. Data reduction

Using standard data reduction software available at Arecibo, the two polarizations were averaged, and corrections were applied for the variations in the gain and system temperature of the telescope with zenith angle and azimuth using the most recent calibration data available at the telescope. Further data analysis was performed using Supermongo routines developed by one of us (SES). A baseline of order zero was fitted to the data, excluding those velocity ranges with HI line emission or radio frequency interference (RFI). Once the baselines were subtracted, the velocities were corrected to the heliocentric system, using the optical convention, and the central line velocity, line widths at, respectively, the 50% and 20% level of peak maximum (Lewis 1983), the integrated flux of the HI profiles, as well as the rms noise of the spectra were determined. All data were boxcar smoothed to a velocity resolution of 14.3 km s^{-1} (velocity search) and 16.4 km s^{-1} (known velocity) for analysis.

The stability of the chain of reception of the Arecibo telescope is known to be good. This is shown by the observations we made of strong continuum sources and of a calibration galaxy with a strong line signal: the latter showed a $\pm 6\%$ standard deviation in its integrated line flux.

4. Results

The global Arecibo HI line data for the observed sample, together with their global near-infrared and optical data, are listed in Tables 3a, b for clearly detected objects, in Tables 4a, b for marginal detections and in Tables 5a, b for undetected objects. A description of all parameters listed in the Tables is given below in Sects. 4.1–4.4. The near-infrared data listed were taken from the 2MASS catalogue and the optical data were taken from the online NED and LEDA databases, as indicated.

The HI spectra of the clearly detected galaxies are shown in Fig. 2 and the marginal detections are shown in Fig. 3; for cases where 2 line profiles were detected in the same spectrum,

designated by “a” and “b” after the 2MASS sourcename, see Sect. 4.5.

The distribution of the integrated line fluxes and FWHM’s of the clear and marginal detections is shown in Fig. 4. Also plotted in this figure is a straight line indicating the 3σ detection limit for a 250 km s^{-1} wide, flat-topped spectral line based on the average rms noise level of the data. The data quality and the rms noise of the Arecibo observations are rather uniform.

4.1. Names, positions and distances

- **Number:** we have divided the selected 2MASS sources according to two criteria: size and algorithm. This division is indicated by two characters in the galaxy designations which we will use throughout this series: an entry starting with “L” indicates a “Large” object with an isophotal K_s -band radius $r_{K_{20}}$ (see Sect. 4.2) larger than $20''$, an “S” a “Small” one with a radius between $10''$ and $20''$ and an “F” a galaxy selected using the LCSB source processor, while following the source number an “O” indicates a previously catalogued object, a “P” one with a PGC entry only and an “N” a previously uncatalogued one.
- **Identifications:** for each of the 2MASS sources we queried the NED and LEDA databases for a cross-identification of its position with other catalogues. For previously catalogued objects we list the most commonly used identification besides the 2MASS identification;
- **Positions:** the column headed “2MASSXi J ” gives the 2MASS source designations, which are the right ascensions and declinations of their centre positions, for epoch J2000.0. These were used as the pointing centres for the HI observations;
- **Distances:** for each detected galaxy, a distance D was calculated using radial HI velocities corrected to the Galactic Standard of Rest, following the RC3 and assuming a Hubble constant of $H_0 = 75 \text{ km s}^{-1} \text{ Mpc}^{-1}$.

4.2. Near-infrared data

- K_{20} is the total magnitude measured within the $r_{K_{20}}$ isophotal aperture (see below);
- $J - K$ is a near-infrared colour of the source, based on magnitudes measured in the J and K_s bands within their respective isophotal semi-major axes at the $20 \text{ mag arcsec}^{-2}$ level;
- μ_{K5} is the mean central surface brightness (in mag arcsec^{-2}) measured within a radius of 5 arcsec around the source’s centre;
- b/a is the infrared axis ratio determined from an ellipse fit to the co-addition of the J -, H -, and K_s -band images. The fit is carried out at the $3\text{-}\sigma$ isophotal level relative to the background noise in each image. The 2MASS F (LCSB sources) sample was not measured in this way because of the low signal-to-noise levels of the emission;
- $r_{K_{20}}$ is the fiducial aperture (in arcsec) in the K_s band. Essentially, it is the aperture size for a surface brightness of $20 \text{ mag arcsec}^{-2}$;
- L_K is the absolute magnitude in the K_s band (in $L_{\odot,K}$), calculated using an absolute solar K_s -band magnitude of 3.33 (Allen 1973).

4.3. Optical data

- $Type$ is the morphological type, as listed in NED or LEDA (the latter are between parenthesis)
- V_{opt} is the mean heliocentric optical radial velocity (in km s^{-1}), as listed in LEDA;
- D_{25} is the isophotal B -band diameter (in units of arcmin) measured at a surface brightness level of $25 \text{ mag arcsec}^{-2}$, as listed in LEDA;
- B_{T_c} is the total apparent B -band magnitude reduced to the RC3 system (de Vaucouleurs et al. 1991) and corrected for galactic extinction, inclination and redshift effects (see Paturel et al. 1997, and references therein), as listed in LEDA;
- $\mu_{B_{25}}$ is the mean B -band surface brightness (in mag arcsec^{-2}) within the $25 \text{ mag arcsec}^{-2}$ isophote, as listed in LEDA;
- L_B is the absolute magnitude in the B band (in $L_{\odot,B}$), calculated using the B_{T_c} magnitude and an absolute solar magnitude in the B band of 5.48 (Allen 1973), as listed in LEDA.

4.4. HI data

The global HI line parameters are directly measured values; no corrections have been applied to them for, e.g., instrumental resolution or cosmological stretching (e.g., Matthews et al. 2001).

- rms is the rms noise level in a spectrum (in mJy);
- I_{HI} is the integrated line flux (in Jy km s^{-1}). The upper limits listed are 3σ values for flat-topped profiles with a width of 250 km s^{-1} , a representative value for the galaxies detected;
- V_{HI} is the heliocentric central radial velocity of a line profile (in km s^{-1}), in the optical convention. We estimated the uncertainty, $\sigma_{V_{\text{HI}}}$ (in km s^{-1}), in V_{HI} following Fouqué et al. (1990), as $\sigma_{V_{\text{HI}}} = 4R^{0.5}P_W^{0.5}X^{-1}$, where R is the instrumental resolution (16.4 km s^{-1} for galaxies with previously known velocity and 14.3 for velocity searches), $P_W = (W_{20} - W_{50})/2$ (in km s^{-1}) and X is the signal-to-noise ratio of a spectrum, which we defined as the ratio of the peak flux density and the rms noise.
- W_{50} and W_{20} are the velocity widths (in km s^{-1}) at 50% and 20% of peak maximum (km s^{-1}), respectively. According to Fouqué et al. (1990), the uncertainty in the linewidths is $2\sigma_{V_{\text{HI}}}$ (see above) for W_{50} and $3\sigma_{V_{\text{HI}}}$ for W_{20} .
- M_{HI} is the total HI mass (in M_{\odot}), $M_{\text{HI}} = 2.356 \times 10^5 D^2 I_{\text{HI}}$, where D is in Mpc and I_{HI} in Jy km s^{-1} ;
- M_{HI}/L_B is the ratio of the total HI mass to the B -band luminosity (in $M_{\odot}/L_{\odot,B}$);
- M_{HI}/L_K is the ratio of the total HI mass to the K_s -band luminosity (in $M_{\odot}/L_{\odot,K}$).

4.5. Notes on individual galaxies

In order to identify sources whose HI detections could have been confused by nearby galaxies, we queried the NED and HyperLeda databases and inspected DSS images over a region of $10'$ radius surrounding the 2MASS position of each source. Although the telescope’s HPBW is $3.6'$ only, an analysis we made of its beam pattern at the time of our observations shows that in the first sidelobe, at $6'$ radius, an estimated 20% of the line flux would be picked up of a $1'$ diameter galaxy,

whereas at about 9/5 radius this percentage has dropped to 0. We also queried these databases for published H I line data of the target galaxies. For further information on galaxies with published H I line parameters, see Sect. 5.2. Quoted values are weighted averages from the HyperLeda database, unless otherwise indicated.

L120: 2MASX J00234816+1441026=UGC 226: UV excess galaxy Mrk 338 (Mazzarella & Balzano 1986), =IRAS F00212+1424.

L190: 2MASX J00323244+2323424=UGC 321: 5 previous H I detections at Arecibo (see Table 2). Optical H α rotation curve in Mathewson & Ford (1996).

S298P: 2MASX J01512494+2235396=PGC 212849: our H I spectrum ($V_{\text{HI}} = 9894 \text{ km s}^{-1}$, $I_{\text{HI}} = 2.3 \text{ Jy km s}^{-1}$, $W_{50} = 348 \text{ km s}^{-1}$) is confused with that of NGC 695, a $B_{\text{T}} = 13.9 \text{ mag}$, $D_{25} = 0.5 \text{ S0?pec}$ galaxy with $V_{\text{opt}} = 9680 \pm 100 \text{ km s}^{-1}$ at 2.6 separation, for which average H I parameters of $V_{\text{HI}} = 9737 \text{ km s}^{-1}$, $I_{\text{HI}} = 5.0 \text{ Jy km s}^{-1}$ and $W_{50} = 250 \text{ km s}^{-1}$ are listed in HyperLeda, which are based on the Arecibo spectra of Garwood et al. (1987), Giovanelli et al. (1986), Lewis (1987) and Mirabel & Sanders (1988). We estimate that about 60% of its line flux will be detected at the position of the target galaxy.

S301O: 2MASX J01545765+3720346=UGC 1380: detected previously in H I at Arecibo (Haynes et al. 1997). H-band photometry (Boselli et al. 2000; Gavazzi et al. 2000).

L81O: 2MASX J01553966+3702188 = CGCG 522-068: H-band photometry (Boselli et al. 2000; Gavazzi et al. 2000). Not detected in our survey.

S490P: 2MASX J03084665+2420483 = PGC 1705247: H I profile partially outside our search range.

L224O: 2MASX J04013761+2449189 = FGC 464/FGC 464b: our H I spectrum of the target galaxy, NGC 464, shows two detections, at 5803 and 6673 km s^{-1} , like the Arecibo spectrum of Giovanelli et al. (1997). At 0.3 from the edge-on Sc galaxy lies another, somewhat smaller, edge-on spiral, FGC 464b. It is impossible to assign the detections to the objects, as neither has a known optical redshift. For the distance dependent parameters listed for L224Oa and L224Ob in Table 4b.1 it was assumed that the H I is associated with NGC 464.

S662P: 2MASX J04040187+1959363 = PGC 1612699: our H I detection ($V_{\text{HI}} = 6553 \text{ km s}^{-1}$, $I_{\text{HI}} = 1.4 \text{ Jy km s}^{-1}$ and $W_{50} = 230 \text{ km s}^{-1}$) is not expected to be significantly confused with that of the S0 IC 358 ($V_{\text{opt}} = 6760 \pm 50 \text{ km s}^{-1}$), at 7.4 separation, since only an estimated 8% of its line flux will be detected at the position of the target galaxy. The Arecibo H I profile of IC 358 (from Giovanelli & Haynes 1993) shows $V_{\text{HI}} = 6770 \text{ km s}^{-1}$, $I_{\text{HI}} = 3.6 \text{ Jy km s}^{-1}$ and $W_{50} = 638 \text{ km s}^{-1}$.

S686O: 2MASX J04140133+2645003 = FGC 470: detected in H I at Nançay (Matthews & van Driel 2000).

L253P: 2MASXI J0447309+242207 = PGC 1705745: H I profile partially outside our search range.

S868P: 2MASX J05221999+1749137 = PGC 1542586: at 2/3, i.e. 1.3 times half the telescope's HPBW from the target galaxy lies IRAS 05192+1745, an Sbc spiral with

$V_{\text{opt}} = 5892 \pm 60 \text{ km s}^{-1}$, $B_{\text{T}} = 16.65 \text{ mag}$ and $D_{25} = 0.8$. As our H I profile parameters are $V_{\text{HI}} = 5559 \text{ km s}^{-1}$ and $W_{50} = 303 \text{ km s}^{-1}$, it does not appear to be confused with the nearby IRAS galaxy.

S766N: 2MASX J04431049+2901446: our H I detection ($V_{\text{HI}} = 6505 \text{ km s}^{-1}$, $I_{\text{HI}} = 1.1 \text{ Jy km s}^{-1}$, $W_{50} = 131 \text{ km s}^{-1}$) is not expected to be significantly confused with that of the S0/a UGC 3142 ($V_{\text{opt}} = 6592 \pm 43 \text{ km s}^{-1}$), at 8.7 separation, since only about 2.5% of its line flux would be detected at the position of the target galaxy. The Arecibo H I profiles of UGC 3142 (from Lu et al. 1990 and Pantoja et al. 1997) show $V_{\text{HI}} = 6496 \text{ km s}^{-1}$, $I_{\text{HI}} = 5.1 \text{ Jy km s}^{-1}$ and $W_{50} = 288 \text{ km s}^{-1}$.

L313O & S1017O: 2MASX J07111558+3110140 & 2MASX J07112782+3111218 = CGCG 146-033 & 146-036, respectively: the two target galaxies are members of an isolated triplet of galaxies, together with CGCG 146-034. Our two H I profiles do not appear to be confused. CGCG 146-034, at $V_{\text{opt}} = 7433 \pm 60 \text{ km s}^{-1}$, has been classified as an elliptical and is therefore likely to be devoid of H I. The 2.9 separation between the two target galaxies is relatively large compared to the telescope's half HPBW of 1.8, and their optical velocities (7515 and 7203 km s^{-1} , respectively) are separated by 313 km s^{-1} . Our H I profiles obtained pointing towards the centres of CGCG 146-033 and CGCG 146-036 in fact do not overlap in velocity: they have, respectively, $V_{\text{HI}} = 7496$ and 7228 km s^{-1} , corresponding well to the optical systemic velocities, and $W_{50} = 163$ and 197 km s^{-1} . The emission seen in spectrum of CGCG 146-036 at $\sim 7450\text{--}7600 \text{ km s}^{-1}$ may be due to CGCG 146-033. The two target 2MASS galaxies are included in the catalogue of nearby poor clusters of galaxies of White et al. (1999).

S1017O: 2MASX J07112782+3111218 = CGCG 148-26: it is quite unlikely that our H I detection ($V_{\text{HI}} = 7181 \text{ km s}^{-1}$, $I_{\text{HI}} = 1.4 \text{ Jy km s}^{-1}$ and $W_{50} = 146 \text{ km s}^{-1}$) of the $B_{\text{T}} = 16.1 \text{ mag}$ target galaxy, without known optical redshift, is confused by the somewhat brighter ($B_{\text{T}} \sim 15.6$) galaxies CGCG 148-33 and 148-34, at about 3' distance, as their optical redshifts of 7516 ± 45 and $7433 \pm 60 \text{ km s}^{-1}$, respectively, are significantly higher. No H I data are available on these two objects.

S1025P: 2MASX J07154721+1930583: it is not possible to determine if our H I detection ($V_{\text{HI}} = 5207 \text{ km s}^{-1}$, $I_{\text{HI}} = 0.43 \text{ Jy km s}^{-1}$ and $W_{50} = 134 \text{ km s}^{-1}$) of the target galaxy is confused with that of a galaxy of similar optical size and brightness, 2MASX J07160231+1932242, at 3.8 distance, since neither has a known optical redshift. At this separation, we estimate that about 30% of line flux of the latter object would be detected at the target position.

S1062O: 2MASX J07471628+2657037 = IC 746: our H I detection appears to be of nearby spiral galaxy NGC 2449, rather than of the target 2MASS object. Our spectrum centered on the 2MASS galaxy shows $V_{\text{HI}} = 4776 \text{ km s}^{-1}$, $I_{\text{HI}} = 1.4 \text{ Jy km s}^{-1}$ and $W_{50} = 248 \text{ km s}^{-1}$, while its optical redshift is 229 km s^{-1} higher, $5005 \pm 39 \text{ km s}^{-1}$. NGC 2449, which lies only 1.5 from the target galaxy and well within the Arecibo HPBW, is an Sab spiral of $B_{\text{T}} = 14.13 \text{ mag}$ and $D_{25} = 1.4$, with $V_{\text{opt}} = 4817 \pm 34 \text{ km s}^{-1}$. A detection of NGC 2449 at Arecibo (Bicay & Giovanelli 1986), shows $V_{\text{HI}} = 4778 \text{ km s}^{-1}$,

$I_{\text{HI}} = 2.0 \text{ Jy km s}^{-1}$ and $W_{50} = 221 \text{ km s}^{-1}$. Two other galaxies of similar redshift, NGC 2449 ($V_{\text{opt}} = 4801 \pm 33 \text{ km s}^{-1}$) and IC 2205 ($V_{\text{opt}} = 4726 \pm 43 \text{ km s}^{-1}$), both about one magnitude fainter in B than NGC 2449, lie about $6'$ from the target galaxy. No HI observations are published of these objects. The target galaxy is included in the catalogue of nearby poor clusters of galaxies of White et al. (1999).

L324O: 2MASX J07480326+2801422=CGCG 148–26: our HI profile ($V_{\text{HI}} = 8041 \text{ km s}^{-1}$, $I_{\text{HI}} = 1.7 \text{ Jy km s}^{-1}$ and $W_{50} = 153 \text{ km s}^{-1}$) of the target galaxy ($V_{\text{opt}} = 8111 \pm 60 \text{ km s}^{-1}$, $B_{\text{T}} = 16.4$) may in principle be confused by a nearby (3.3 separation), somewhat more luminous galaxy galaxy, CGCG 148–28 ($V_{\text{opt}} = 8163 \pm 43 \text{ km s}^{-1}$, $B_{\text{T}} = 15.6$), both without published morphological type. At this separation, we expect that about 40% of the line flux of the latter would be detected at the position of the target galaxy.

S1080O: 2MASX J07551046+1422131 = CGCG 58–70: there will be no confusion of our detection at $V_{\text{HI}} = 13446 \text{ km s}^{-1}$ of the target galaxy ($V_{\text{opt}} = 13447 \text{ km s}^{-1}$) with the three similarly bright galaxies at about $4'$ to 7.5 distance (CGCG 58–68, –69 and –71), since these all have optical redshifts of $\sim 8750 \text{ km s}^{-1}$.

L363O: 2MASX J09030837+1739356=FGC 828: since none have optical redshifts, it is impossible to determine if our HI detection ($V_{\text{HI}} = 8832 \text{ km s}^{-1}$, $I_{\text{HI}} = 1.0 \text{ Jy km s}^{-1}$ and $W_{50} = 158 \text{ km s}^{-1}$) of the target galaxy, with $K_{20} = 12.5$, is confused by 2 smaller nearby 2MASS galaxies, 2MASX J09030383+1741336 of $K_{20} = 12.8$ at 2.3 distance, and 2MASX J09031111+1740431 of $K_{20} = 14.4$ at 1.4 distance. At these separations, we estimate that about 70% to 90% of the galaxy pair CGCG 90–59, at 6.5 distance, has a much higher redshift of about 16000 km s^{-1} .

S1283O: 2MASX J09223543+2051068=PGC 86616: detected previously in HI at Arecibo (Schombert et al. 1992).

S1317O: 2MASXI J0939167+321838=NGC 2944 pair: interacting galaxy pair (=Arp 63). The separation of NGC 2944 into two galaxies is best seen on the 2MASS images, where the projected distance of their nuclei is $16''$, as the DSS image is saturated in the inner regions. The selected 2MASS source corresponds to the centre of the least bright, W nucleus. Optical spectroscopy (Maehara et al. 1987) only showed $\text{H}\alpha$ + $[\text{NII}]$ emission lines, with an equivalent width of 57 \AA for $\text{H}\alpha$. $28''$ SE of the centre of the NGC 2944 pair lies PGC 27534, a $B_{\text{T}} = 16$: object of $D_{25} = 0.2$ without published optical redshift. NGC 2944 was detected previously in HI at Arecibo (Williams & Kerr 1981) and at Nançay, (Chamaraux 1977). The central HI velocities measured at the two telescope differ significantly: 6783 and 6753 km s^{-1} at Arecibo compared to 6831 km s^{-1} at Nançay. The much higher Nançay I_{HI} of $13.6 \text{ Jy km s}^{-1}$ compared to the 4.0 Jy km s^{-1} we measured at Arecibo can be explained partially by confusion within the larger Nançay beam with the interacting UGC 5146 pair (=Arp 129), at 3.7 separation, for which Bica & Giovanelli (1986) measured at Arecibo $V_{\text{HI}} = 6862$, $I_{\text{HI}} = 4.8 \text{ Jy km s}^{-1}$ and $W_{50} = 163 \text{ km s}^{-1}$. The W_{50} width we measured at Arecibo is almost twice the value measured by Williams & Kerr, 149 km s^{-1} .

L388O: 2MASX J09403295+2529255 = UGC 5156: its optical redshift is $10028 \pm 43 \text{ km s}^{-1}$. It was detected previously in HI at Arecibo (Bica & Giovanelli 1986), at $V_{\text{HI}} = 9953 \text{ km s}^{-1}$, 174 km s^{-1} higher than our central velocity, which appears to be due to the fact that our HI profile lies partially outside the search range. At 5.8 distance lies a galaxy of similar redshift ($V_{\text{opt}} = 10082 \pm 43 \text{ km s}^{-1}$), size, magnitude and high inclination, CGCG 122–47. The HI profiles may in principle be confused by this object, as we estimate that about 25% of its line flux would be detected at the target position.

S1342O: 2MASX J09501016+3424534=KUG 0947+346: its optical velocity, $6590 \pm 47 \text{ km s}^{-1}$ (Kowal et al. 1974) is about 1000 km s^{-1} lower than our HI velocity, 7571 km s^{-1} . At 7.1 distance lies a somewhat brighter Sc spiral, KUG 0946+346, of unknown redshift. Since we estimate that only about 15% of its line flux would be detected at the target position, it does not seem likely that the HI profile is confused by it.

S1357O: 2MASX J09560425+1630537=LSBC F637–01: our HI detection ($V_{\text{HI}} = 3825 \text{ km s}^{-1}$, $I_{\text{HI}} = 1.2 \text{ Jy km s}^{-1}$ and $W_{50} = 130 \text{ km s}^{-1}$) is not expected to be significantly confused by the SBa NGC 3053 ($V_{\text{opt}} = 3774 \pm 60 \text{ km s}^{-1}$), at 8.8 separation, since only an estimated 2.5% of its line flux will be detected at the target position. The Arecibo HI profiles of NGC 3053 (Chengalur et al. 1993; Giovanardi & Salpeter 1985) show $V_{\text{HI}} = 3730 \text{ km s}^{-1}$, $I_{\text{HI}} = 4.3 \text{ Jy km s}^{-1}$ and $W_{50} = 409 \text{ km s}^{-1}$.

S2687P: 2MASX J22401444+3438401=PGC 2052363: our HI profile ($V_{\text{HI}} = 8404 \text{ km s}^{-1}$, $I_{\text{HI}} = 2.6 \text{ Jy km s}^{-1}$, $W_{50} = 226 \text{ km s}^{-1}$) may in principle be confused by the galaxy 2MASX J22404656+3437520 at 6.4 distance, which is 1.2 mag brighter in the K_s band. Neither have an optical redshift. Only about an estimated 15% of its line flux would be detected at the target position.

S2730P: 2MASX J22551306+3248080=PGC 2012878: our HI profile may be a detection of nearby galaxy Ark 569, an SBbc spiral with $B_{\text{T}} = 15.6$ and $D_{25} = 0.8$ without a known optical redshift. At 4.3 distance, we estimate that about 30% of its line flux would be detected at the target position. An Arecibo detection (Giovanelli & Haynes 1985) of Ark 569 shows $V_{\text{HI}} = 6000 \text{ km s}^{-1}$ and $W_{50} = 266 \text{ km s}^{-1}$, values very close to the $V_{\text{HI}} = 6018 \text{ km s}^{-1}$ and $W_{50} = 270 \text{ km s}^{-1}$ we measured pointing towards the 2MASS object. The integrated HI line flux we measured towards the 2MASS galaxy, 0.4 Jy km s^{-1} , is 10 times smaller than the 4.0 Jy km s^{-1} measured towards Ark 569.

L802P: 2MASX J22580271+3227586=PGC 2800849: detected previously in HI at Arecibo (Cabanela & Dickey 1999), with $V_{\text{HI}} = 6588 \text{ km s}^{-1}$ and $I_{\text{HI}} = 1.5 \text{ Jy km s}^{-1}$, and an average of the W_{50} and W_{20} line widths of 283 km s^{-1} . Surprisingly, the object was not detected in our survey, with an rms noise level of 1.19 mJy . For a flat-topped profile with width of 283 km s^{-1} , this would imply a 3σ upper limit to I_{HI} of 1.0 Jy km s^{-1} , well below the value measured previously.

L807O: 2MASX J22594147+2404297 = UGC 12289: our HI profile of the target galaxy ($V_{\text{HI}} = 9986 \text{ km s}^{-1}$, $W_{50} = 217 \text{ km s}^{-1}$, $I_{\text{HI}} = 4.3 \text{ Jy km s}^{-1}$), with $V_{\text{opt}} = 10160 \pm 42 \text{ km s}^{-1}$, lies partially outside our search range,

which explains the 174 km s^{-1} difference with the optical redshift and the Arecibo detection by Giovanelli et al. (1986), which shows $V_{\text{HI}} = 10\,160 \text{ km s}^{-1}$, $W_{50} = 218 \text{ km s}^{-1}$ and $I_{\text{HI}} = 3.1 \text{ Jy km s}^{-1}$. The profile is not expected to be confused significantly by the $B_{\text{T}} 16.1$ SBab spiral UGC 12283, with $V_{\text{opt}} = 9949 \pm 60 \text{ km s}^{-1}$, which was detected at Arecibo by Giovanelli et al. (1986), who found $V_{\text{HI}} = 9949 \text{ km s}^{-1}$, $W_{50} = 274 \text{ km s}^{-1}$ and $I_{\text{HI}} = 0.7 \text{ Jy km s}^{-1}$. At 5:3 distance, we estimate that about 25% of its line flux would be detected at the target position.

L8150: 2MASX J23145953+1459192=MCG 02-59-12: our HI detection ($V_{\text{HI}} = 11\,908 \text{ km s}^{-1}$, $I_{\text{HI}} = 0.95 \text{ Jy km s}^{-1}$, $W_{50} = 48 \text{ km s}^{-1}$) of the target galaxy, which has an optical redshift of $12\,182 \pm 60 \text{ km s}^{-1}$, may in principle be confused by two nearby objects: a $B = 16$ mag object without a PGC entry at $23^{\text{h}}15^{\text{m}}12^{\text{s}}.2$, $14^{\circ}58'22''$ at $12\,182 \text{ km s}^{-1}$ and 3:2 distance, and $B_{\text{T}} = 16.2$ mag Sc spiral UGC 12448 at $11\,955 \text{ km s}^{-1}$ and 6:4 distance. At these separations, we estimate that about 40% and 20%, respectively, of their line fluxes would be detected at the target position.

S28170: 2MASXI J2323068+124955 = KUG 2320+125: B and R -band CCD imaging and long-slit spectroscopy (Grogin & Geller 1999, 2000).

L8290: 2MASXI J2347570+280747 = FGC 2536: detected in HI at Nançay (Matthews & van Driel 2000).

S28340: 2MASX J23343591+2353362= KUG 2332+236: two HI lines were detected in our spectrum, at 5615 and 9802 km s^{-1} , respectively. The $B_{\text{T}} = 16.5$ Sc-type target galaxy has no known optical redshift. For the distance dependent parameters listed for S28340a and b in Table 4b.2 it was assumed that the HI is associated with the target galaxy. Our lower velocity detection ($V_{\text{HI}} = 5615 \text{ km s}^{-1}$, $I_{\text{HI}} = 0.9 \text{ Jy km s}^{-1}$, $W_{50} = 298 \text{ km s}^{-1}$) will be completely confused by two nearby galaxies, both without known optical redshift, which were detected in HI at Arecibo by Spitzak & Schneider (1998): the $B_{\text{T}} = 17.3$ mag PGC 169947 ($V_{\text{HI}} = 5603 \text{ km s}^{-1}$, $I_{\text{HI}} = 1.7 \text{ Jy km s}^{-1}$, $W_{50} = 162 \text{ km s}^{-1}$) at 2:1, and the $B_{\text{T}} = 17.6$ mag PGC 169948 ($V_{\text{HI}} = 5558 \text{ km s}^{-1}$, $I_{\text{HI}} = 2.7 \text{ Jy km s}^{-1}$, $W_{50} = 109 \text{ km s}^{-1}$) at 5:1 distance. We estimate that about 75% of the line flux of the former and about 25% of the flux of the latter would be detected at the target position, i.e. in total about 2 Jy km s^{-1} - twice the total flux we measured.

5. Discussion

5.1. Comparison with published HI data

Of the 127 galaxies we detected at 21 cm, 10 were detected previously in HI (see Sect. 4.5 and Table 2). Of these, 7 were detected at Arecibo only, one at both Arecibo and Nançay (NGC 2944) and 2 at Nançay only (FGC 470 and 2536). Basically all published Arecibo measurements were made before its major upgrade, while ours were made after. A comparison of these data with ours generally shows good agreement, except for the case of the confused Nançay profile of the interacting pair NGC 2944 (S13170) and for UGC 12289 (L8070), where our profile lies partially outside the band (see Sect. 4.5).

Excluding NGC 2944 and UGC 12289, the average absolute value and its σ_N deviation of the differences between our radial velocities and the published HI velocities is $25 \pm 21 \text{ km s}^{-1}$, compared to the average estimated uncertainty of 6 km s^{-1} in the values we measured for these objects, while the average ratio of our W_{50} line widths and the published values is 1.02 ± 0.06 , and the ratio of the integrated line fluxes is 0.82 ± 0.17 .

5.2. Radio Frequency Interference (RFI)

As a consequence of their high sensitivity, radio astronomy telescopes are vulnerable to radio frequency interference (RFI), with signal strengths usually greatly exceeding those of the weak celestial radio sources being observed. Broad-band RFI raises the noise level of the observations, while narrow-band RFI may mimic spectral lines like the HI lines from galaxies that are being searched for in the present study.

It should be noted that in the ITU-R Radio Regulations (2001), with which all users of the radio spectrum are obliged to comply, astronomical HI line observations are only protected from “all emissions” up to a redshift of about 4300 km s^{-1} , while for observations further out to $\sim 19\,000 \text{ km s}^{-1}$ “(national frequency) administrations are urged to take all practicable steps to protect the radio astronomy service from harmful interference”. These regulatory provisions for the protection of the Radio Astronomy Service clearly cannot guarantee a completely RFI-free environment for the kind of survey we performed.

Though care was taken to make the renovated Arecibo telescope more robust for unwanted radio interference (RFI), and to coordinate its operation as well as possible with the frequency plan and emission periods of local radar installations, persistent RFI signals with strengths that make the detection of faint HI line signals impossible were present during a significant fraction of the observations.

In order to examine during what percentage of time which radial velocity ranges are interfered with, considering the faintness of the line signals we are searching for, we flagged all channels in all spectra made in the velocity search mode (see Sect. 3.1) showing signals with a flux density exceeding the 20 mJy level after baseline fitting – a level exceeded by only two of our 107 detected galaxies: S622P at $11\,711 \text{ km s}^{-1}$ and L8070 at 9986 km s^{-1} . Plots of the relative number of times such signals occurred during the November 2000 and January 2001 observing runs are shown in Fig. 1, in bins with a width of 25 km s^{-1} (about 10 channels). Besides RFI, the plots show the omnipresent Galactic HI emission around 0 km s^{-1} . The most troublesome RFI signal in the velocity searches, of which about 85% were made in the -500 to $11\,000 \text{ km s}^{-1}$ range, are the intermittent GPS L3 emissions in the $\sim 81\,500 - 8700 \text{ km s}^{-1}$ range (around 1381 MHz): 12% of all spectra showed RFI exceeding the 20 mJy level in this range.

6. Conclusions

Of the 367 galaxies observed, 127 (35%) were clearly detected, 66 of which did not have a previously known radial velocity.

Table 1. Detection statistics.

	Previously Catalogued (Other)			Previously Catalogued (PGC)			Previously Uncatalogued (New)		
	Large	Small	Faint	Large	Small	Faint	Large	Small	Faint
Total observed	25	75	1	14	179	0	17	55	1
Detected	19	37	1	8	27	0	12	2	1
Marginal	2	7	0	0	8	0	3	0	0
Undetected	4	31	0	6	144	0	2	53	0
Det.+Margin.	21	44	1	8	35	0	15	2	1
	84%	59%	100%	57%	20%	–	88%	4%	100%

Note: large: $r_{K_{20}} \geq 20''$, small: $20'' \geq r_{K_{20}} \geq 10''$, faint: galaxies selected with the LCSB source processor.

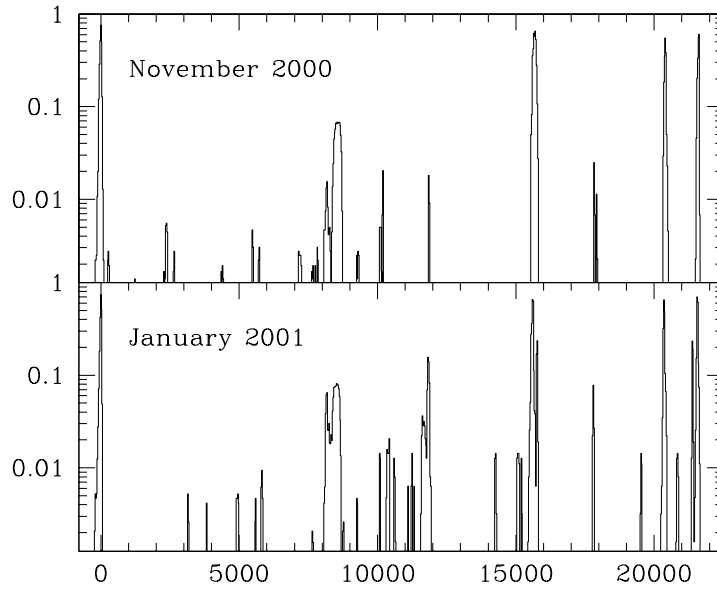


Fig. 1. Plots showing the relative occurrence of radio frequency interference (RFI) during the two observing runs, for the observations made in the velocity search mode (see Sect. 3.1). It also shows the omnipresence of Galactic HI emission around 0 km s^{-1} . Shown as function of radial velocity is the relative number of spectra with signals having a flux density exceeding the 20 mJy level, in 25 km s^{-1} wide bins.

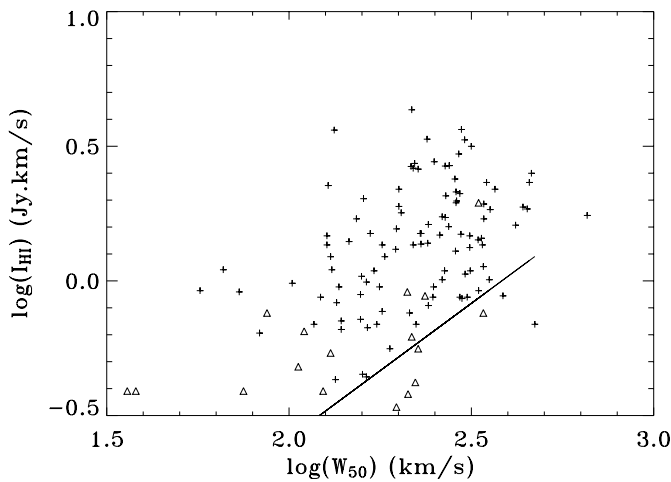


Fig. 4. Distribution of integrated HI line fluxes (I_{HI}) as a function of the HI line FWHM, W_{50} . The straight line indicates the 3σ detection limit for a 250 km s^{-1} wide, flat-topped spectral line, based on the average rms noise level of the data. Clear detections are represented by crosses, marginal detections by triangles.

The detection statistics as function of type (previously catalogued, PGC entry only or uncatalogued) and size or selection algorithm (large/small/faint) are listed in Table 1. For the Large objects ($r_{K_{20}} \geq 20''$) the global detection rate (for both

previously catalogued and uncatalogued objects) is 79%, while for the small objects ($20'' \geq r_{K_{20}} \geq 10''$), the global detection rate is much lower, 26%.

Table 3a.1. Detected objects – identifications and coordinates.

Number	2MASS hhmss.s+ddmmss (J2000.0)	PGC	others
S44O	0020308+383418	1312	CGCG 518–023
L12O	0023481+144101	1511	UGC 226
L19O	0032324+232342	1971	UGC 321
(F1O)	0037501+172258	2256	CGCG 457–023
S243O	0131243+313045	5668	KUG 0128+3122
S298P	0151249+223539	212849	
S301O	0154576+372034	7124	UGC 1380
S384P	0225148+270156	1795794	
S389P	0226467+244228	1714313	
S396N	0229235+280905		
L122P	0233244+202330	1625902	
L123O	0233281+220753	1664146	CGCG 484–009B
S447P	0249372+355358	2071747	
S452O	0253357+255645	10920	MCG 04-07-029
L146N	0257297+195708		
S474P	0302524+162718	1509176	
L160O	0305530+160701	11630	UGC 2532
S490P	0308466+242048	1705247	
L166P	0309401+365421	2089118	
S502P	0310312+191406	1585156	
S503N	0310370+210938		
S529P	0316488+270654	1798183	
(F10N)	0320157+370635		
S546N	0322247+294309		
L183P	0323427+143037	1460054	
S550N	0323598+121455		
L185P	0324146+330920	2024928	
S597P	0338269+124840	1416658	
S604O	0339347+204231	1634156	NPM1G 20.0119
S611P	0342200+300939	1892676	
S622P	0348449+122942	1410586	
L216O	0350531+373637	13961	UGC 2876
S638P	0355096+282040	1833185	
L221P	0355478+164649	1516836	
L224O	0401376+244919	90699	FGC 464b
S662P	0404018+195936	1612699	
S679N	0412357+254402		
S683N	0413211+361816		
S686O	0414013+264500	90703	FGC 470
S708N	0422078+351728		
S766N	0443104+290143		
L250N	0445255+182505		
L253P	0447309+242207	1705745	
S785N	0449068+171009		
S791N	0451218+271254		
S792P	0451312+173814	1537658	
L273P	0517166+120504	1403526	
S868P	0522199+174913	1542586	
S1015P	0711116+233146	1688965	
L131O	0711155+311014	20346	CGCG 146–033
S1017O	0711278+311121	20355	CGCG 146–036
S1025P	0715472+193058	1595261	
S1043O	0732327+361206	21241	KUG 0729+363
S1047P	0735148+230634	1681613	
S1050O	0739291+181044	21504	CGCG 087–025
S1058P	0745277+341023	2045032	
S1061P	0747033+181120	1552617	
S1062O	0747163+265703	21796	IC 476
L324O	0748032+280141	21835	CGCG 148–026
S1074P	0753295+140122	1447100	
S1080O	0755104+142213	0022178	CGCG 058–070
S1083O	0756250+292809	0022241	CGCG 148–070
(S1090O)	0800463+294452	0022472	CGCG 148–090
L331O	0802121+321854	22545	KUG 0759+324
S1099O	0805041+294321	0022688	CGCG 148–109
S1138O	0823396+181800	0023554	CGCG 089–013
S1141O	0824171+302908	0023583	KUG 0821+306
S1155P	0829353+192901	1593979	
S1157O	0830541+201452	0023882	CGCG 089–038
S1158O	0832194+311127	0023946	KUG 0829+313
S1192O	0847070+275224	0024677	CGCG 150–030

Table 3a.2. continued.

Number	2MASS hhmss.s+ddmmss (J2000.0)	PGC	others
S1194O	0848176+165733	24738	CGCG 090–013
S1226O	0901122+130240	25336	CGCG 061–039
L363O	0903081+173932	90887	FGC 828
L368O	0913163+312130	25984	CGCG 151–023
S1275O	0919588+171617	26393	CGCG 091–071
S1283O	0922354+205106	86616	LSBC F565–01
L381O	0929175+302302	26915	CGCG 152–016
L384O	0935217+133255	27259	CGCG 063–015
S1310O	0936142+172905	27320	CGCG 092–009
S1317O	0939167+321838	27534	KUG 0936+325A
L388O	0940332+252921	27615	UGC 5156
S1323O	0940379+193449	27618	CGCG 092–027
S1326O	0942002+192507	27710	CGCG 092–031
S1333O	0945454+335212	27987	UGC 5217
S1342O	0950100+342453	28304	KUG 0947+346
S1345O	0951538+145555	28409	CGCG 092–059
S1357O	0956042+163053	1510621	LSBC F637–01
L422P	1033536+240119	31233	
S1459O	1045268+214853	1657843	IRAS F10427+2204
S1494N	1102452+195439		
S2501P	2041579+142054	1455783	
L756O	2052005+132950	65594	CGCG 425–015
S2534O	2103403+165219	1519091	NPM1G 16.0496
S2569P	2125131+311932	1941957	
S2596N	2147348+130514		
L790O	2230502+363348	69034	CGCG 514–048
S2687P	2240144+343840	2052363	
S2710P	2248274+334421	2037938	
S2734P	2257091+131117	70087	
L807O	2259414+240429	70197	UGC 12289
L815O	2314595+145919	70809	MCG 02-59-012
S2810O	2321027+151319	86491	KUG 2318+149
S2817O	2323068+124955	71279	KUG 2320+125
S2834O	2334359+235335	85503	KUG 2332+236
L829O	2347570+280747	91822	FGC 2536
S2893O	2357258+265018	85905	KUG 2354+265

No: source names in brackets are not found in later versions of the public 2MASS database.

Acknowledgements. This publication makes use of data products from the Two Micron All Sky Survey, which is a joint project of the University of Massachusetts and the Infrared Processing and Analysis Center, funded by the National Aeronautics and Space Administration and the National Science Foundation. We also wish to thank the Arecibo Observatory which is part of the National Astronomy and Ionosphere Center, which is operated by Cornell University under a cooperative agreement with the National Science Foundation. This research also has made use of the Lyon-Meudon Extragalactic Database (LEDA), recently incorporated in HyperLeda, the NASA/IPAC Extragalactic Database (NED) which is operated by the Jet Propulsion Laboratory, California Institute of Technology, under contract with the National Aeronautics and Space Administration and the Aladin database, operated at CDS, Strasbourg, France. We acknowledge financial support from CNRS/NSF collaboration grant No. 10637 and from the ASTE of CNRS/INSU.

References

- Allen, C. W. 1973, *Astrophysical Quantities* (London: Athlone Press)
- Bicay, M. D., & Giovanelli, R. 1986, *AJ*, 91, 732
- Bohringer, H., Voges, W., Huchra, J. P., et al. 2000, *ApJS*, 129, 435
- Boissier, N., Prantzos, N., Monnier Ragaigine, D., et al. 2003, *MNRAS*, in press [astro-ph/0304313]
- Boselli, A., Gavazzi, G., Franzetti, P., Pierini, D., & Scodreggio, M. 2000, *A&AS*, 142, 73
- Bothun, G. D., Impey, C. D., Malin, D. F., & Mould, J. R. 1987, *AJ*, 94, 23
- Cabanela, J. E., & Dickey, J. M. 1999, *AJ*, 118, 46
- Chamaraux, P. 1977, *A&A*, 60, 67
- Chengalur, J. N., Salpeter, E. E., & Terzian, Y. 1993, *ApJ*, 419, 30
- Chung, A., van Gorkom, J. H., O'Neil, K., & Bothun, G. D. 2002, *AJ*, 123, 2387
- de Blok, W. J. G., McGaugh, S. S., & van der Hulst, J. M. 1996, *MNRAS*, 283, 18
- de Vaucouleurs, G., de Vaucouleurs, A., Corwin, H. G., et al. 1991, *The Third Reference Catalogue of Bright Galaxies* (New York: Springer-Verlag) (RC3)
- Fouqué, P., Bottinelli, L., Durand, N., Gouguenheim, L., & Paturel, G. 1990, *A&AS*, 86, 473
- Garwood, R. W., Helou, G., & Dickey, J. M. 1987, *ApJ*, 322, 88
- Gavazzi, G., Franzetti, P., Scodreggio, M., Boselli, A., & Pierini, D. 2000, *A&A*, 361, 863
- Giovanardi, C., & Salpeter, E. E. 1985, *ApJS*, 58, 623
- Giovanelli, R., & Haynes, M. P. 1985, *AJ*, 90, 2445
- Giovanelli, R., Haynes, M. P., Myers, S. T., & Roth, J. 1986, *AJ*, 92, 250
- Giovanelli, R., & Haynes, M. P. 1993, *AJ*, 105, 1271
- Giovanelli, R., Avera, E., & Karachentsev, I. D. 1997, *AJ*, 114, 122
- Grogin, N. A., & Geller, M. J. 1999, *AJ*, 118, 2561
- Grogin, N. A., & Geller, M. J. 2000, *AJ*, 119, 32
- Haynes, M. P., Giovanelli, R., Herter, T., et al. 1997, *AJ*, 113, 1197
- Haynes, M. P., Giovanelli, R., Chamaraux, P., et al. 1999, *AJ*, 117, 2039
- Hurt, R. L., Jarrett, T. H., Kirkpatrick, J. D., et al. 2000, *AJ*, 120, 1876
- ITU-R Radio Regulations 2001, International Telecommunication Union (ITU, Geneva)
- Jarrett, T. H., Chester, T., Cutri, R., et al. 2000a, *AJ*, 119, 2498
- Jarrett, T. H., Chester, T., Cutri, R., et al. 2000b, *AJ*, 120, 298
- Kowal, C. T., Zwicky, F., Sargent, W. L. W., & Searle, L. 1974, *PASP*, 86, 516
- Lewis, B. M. 1983, *AJ*, 88, 962
- Lewis, B. M. 1987, *ApJS*, 63, 515
- Lu, N. Y., Dow, M. W., Houck, J. R., Salpeter, E. E., & Lewis, B. M. 1990, *ApJ*, 357, 388
- Mathewson, D. S., & Ford, V. L. 1996, *ApJS*, 107, 97
- Matthews, L. D., & van Driel, W. 2000, *A&A*, 143, 421
- Matthews, L. D., van Driel, W., & Monnier-Ragaigine, D. 2001, *A&A*, 365, 1
- Mazzarella, J. M., & Balzano, V. A. 1986, *ApJS*, 62, 751
- McGaugh, S. S., & de Blok, W. J. G. 1997, *ApJ*, 481, 689
- McGaugh, S. S., Rubin, V. C., & de Blok, W. J. G. 2001, *AJ*, 122, 2381
- Mirabel, I. F., & Sanders, D. B. 1988, *ApJ*, 335, 104
- Monnier Ragaigine, D., van Driel, W., Schneider, S. E., Jarrett, T. H., & Balkowski, C. 2003a, *A&A*, 405, 99 (Paper I)
- Monnier Ragaigine, D., van Driel, W., Schneider, S. E., Balkowski, C., & Jarrett, T. H. 2003b, *A&A*, in press (Paper III)
- Monnier Ragaigine, D., Papaderos, P., van Driel, W., et al. 2003c, *A&A*, in preparation (Paper IV)
- O'Neil, K., Bothun, G. D., Schombert, J., Cornell, M. E., & Impey, C. D. 1997, *AJ*, 114, 2448
- O'Neil, K., Bothun, G. D., & Schombert, J. 2000, *AJ*, 119, 136
- Pantoja, C. A., Altschuler, D. R., Giovanardi, C., & Giovanelli, R. 1997, *AJ*, 113, 905
- Paturel, G., Bottinelli, L., Di Nella, H., et al. 1997, *A&AS*, 124, 109
- Schneider, S., Huchra, J., Jarrett, T., & Chester, T. 1997, *2MASS Extragalactic Studies: Early Results from the Prototype Camera*, in *The Impact of Large-Scale Near-IR Sky Surveys*, ed. F. Garzón, N. Epchtein, A. Omont, W. B. Burton, & P. Persi (Dordrecht: Kluwer), 231
- Spitzak, J. G., & Schneider, S. E. 1992, *ApJ*, 393, 126
- Spitzak, J. G., & Schneider, S. E. 1998, *ApJS*, 119, 159
- Theureau, G., Bottinelli, L., Coudreau-Durand, N., et al. 1998, *A&AS*, 130, 333
- van den Hoek, L. B., de Blok, W. J. G., van der Hulst, J. M., & de Jong, T. 2000, *A&A*, 357, 397
- van der Hulst, J. M., Skillman, E. D., Smith, T. R., et al. 1993, *AJ*, 106, 548
- van Zee, L., Haynes, M. P., & Salzer, J. J. 1997, *Star Formation Activity in High M/L Galaxies*, in *Dwarf Galaxies: Probes for galaxy formation and Evolution*, IAU GA Joint Discussion, Kyoto, Japan, 14
- White, R. A., Bliton, M., Bhavsar, S. P., et al. 1999, *AJ*, 118, 2014
- Williams, B. A., & Kerr, F. J. 1981, *AJ*, 86, 953

Online Material

Table 2. Comparison with published HI data.

No.	Ident.	V_{HI} km s ⁻¹	I_{HI} $\frac{\text{Jy km}}{\text{s}}$	W_{50} km s ⁻¹	Tel.	Ref.
L190	UGC 321	4655	2.6	219	A	this paper
		4668	3.7	233	A	Giovanelli et al. (1986)
		4668	–	220	A	Mathewson & Ford (1996)
		4658	4.7	213	A	Spitzak & Schneider (1998)
		4665	3.7	213	A	Haynes et al. (1999)
F10	MCG 03-02-019	5500	0.94	160	A	this paper
		5510	1.1	–	A	Giovanelli & Haynes (1993)
S301O	UGC 1380	4548	0.89	157	A	this paper
		4601	0.90	166	A	Haynes et al. (1997)
L224Oa	FGC464/464b	5803	1.2	269	A	this paper
		5801	1.5	259	A	Giovanelli et al. (1997)
L224Ob	FGC464/464b	6673	1.7	203	A	this paper
		6674	1.6	215	A	Giovanelli et al. (1997)
S686O	FGC 470	5552	3.4	239	A	this paper
		5555	3.2	240	N	Matthews & van Driel (2000)
S1283O	PGC 86616	9430	1.4	337	A	this paper
		9486	2.1	339	A	Schombert et al. (1992)
S1317O	NGC 2944	6783	3.6	297	A	this paper
		6753	3.4	149	A	Williams & Kerr (1981)
		6831	13.6	–	N	Chamaraux et al. (1977)
L388O	UGC 5156	9896	1.9	438	A	this paper
		9953	2.4	425	A	Bicay & Giovanelli (1986)
L829O	FGC 2536	9207	2.2	367	A	this paper
		9236	2.5	343	N	Matthews & van Driel (2000)

Telescope codes:

A Arecibo

N Nançay

Table 4a. Marginal detections – identifications and coordinates.

Number	2MASS hhmmss.s+ddmmss (J2000.0)	PGC	others
S137P	0055337+294438	1876630	
S370N	0219284+164731		
S388O	0225429+284034	9223	KUG 0222+284
S446P	0248590+151241	1478344	
S658P	0402598+134515	1439552	
S676N	0409533+243427		
S1035O	0721585+292950	20814	CGCG 147–013
S1086P	0758032+144144	1464653	
S1100O	0805478+301350	22726	CGCG 148–111
S1206O	0855023+264031	25028	CGCG 150–045
S1243O	0907047+360646	86893	KUG 0903+363B
S1259P	0915232+312107	1943146	
L383O	0929352+243525	26944	CGCG 122–004
S1303O	0932452+333820	82424	KUG 0929+338
S1311O	0936581+311952	27367	KUG 0934+315A
L386O	0938557+354141	82492	KUG 0935+359
S2730P	2255130+324808	2012878	
L822O	2325102+121820	71383	CGCG 431–060
S2823P	2328052+173440	1536138	
S2851P	2340459+263318	93864	
S2877N	2352344+163651		

Table 4b. Marginal detections – basic data.

No	K_{20}	$J - K$	μ_{K5}	b/a	r_{K20}	B_{Tc}	D_{25}	μ_{B25}	T	rms	I_{HI}	V_{HI}	V_{opt}	W_{50}	D	M_{HI}	L_K	L_B	$\frac{M_{HI}}{L_K}$	$\frac{M_{HI}}{L_B}$
	mag	mag	$\frac{\text{mag}}{m^2}$	"	mag	'	$\frac{\text{mag}}{m^2}$			mJy	$\frac{\text{Jy km}}{\text{s}}$	km s^{-1}	km s^{-1}	km s^{-1}	Mpc	[log] M_{\odot}	[log] $L_{\odot,K}$	[log] $L_{\odot,B}$		
S137P	13.41	1.12	19.03	0.30	16.4	16.60	0.74	25.01		1.24	0.88	5107		236	68.1	8.98	9.67	9.22	0.21	0.58
S370N	12.79	1.12	18.86	0.34	11.6					0.83	0.48	4466		106	59.5	8.60	9.79		0.06	
S388O	13.47	1.07	18.18	0.38	14.4	16.00	0.58	24.01		0.95	0.65	10 097		110	134.6	9.44	10.23	10.05	0.16	0.25
S446P	12.73	1.04	19.07	0.35	14.0	16.80	0.48	24.30		1.32	0.76	14 521		341	193.6	9.83	10.84	10.04	0.10	0.61
S658P	13.52	1.19	18.15	0.36	11.2	16.70	0.63	25.63		0.91	0.39	9392		124	125.2	9.16	10.15	9.71	0.10	0.28
S676N	12.78	1.30	18.78	0.66	10.6					0.70	0.27	6008		191	204	8.61	10.06		0.04	
S1035O	12.22	0.96	18.08	0.77	14.8	15.60	0.63	23.61	Sm	0.87	0.38	7932	7809	212	105.7	9.00	10.52	9.99	0.03	0.10
S1086P	13.26	1.34	18.86	0.56	12.6	16.50	0.50	23.89		0.75	0.29	1355		148	18.0	7.35	8.57	8.10	0.06	0.18
S1100O	12.22	0.96	18.45	0.32	17.2	15.17	0.87	23.67	(Sb)	1.18	0.39	2270	2330	75	30.2	7.92	9.43	9.08	0.03	0.07
S1206O	13.22	1.65	18.35	0.56	11.8	15.89	0.46	23.08	(SBc)	0.79	0.54	8013	8198	130	106.8	9.16	10.13	9.89	0.11	0.19
S1243O	12.88	0.90	18.32	0.40	14.4	15.70	0.72	23.76	S	0.98	0.68	7334		47	97.7	9.19	10.19	9.89	0.10	0.20
S1259P	12.77	0.96	18.26	0.88	13.2	17.30	0.40	24.18		0.99	0.39	1847		36	24.6	7.74	9.02	8.03	0.05	0.51
L383O	12.74	1.08	18.02	0.30	22.0	15.75	0.93	24.42		1.21	1.95	9167		331	122.2	9.84	10.44	10.06	0.25	0.60
S1303O	12.95	1.12	18.57	0.92	11.2	16.14	0.58	23.76	S	1.20	0.91	8118		211	108.2	9.40	10.25	9.80	0.14	0.40
S1311O	12.11	1.07	18.74	0.74	14.6	15.54	0.78	23.83	S	1.32	0.62	7956	8055	217	106.0	9.22	10.57	10.03	0.04	0.16
L386O	13.00	0.91	18.13	0.30	20.4	15.15	0.74	23.19	S	1.46	0.76	6033		87	80.4	9.06	9.97	9.94	0.12	0.13
S2730P	13.02	0.96	18.47	0.32	14.2	16.30	0.69	24.70		0.80	0.42	6094		222	81.2	8.82	9.97	9.49	0.07	0.21
L822O	12.56	1.22	18.21	0.54	22.0	15.07	0.66	23.19		1.08	0.34	3749	3808	197	50.0	8.30	9.74	9.56	0.04	0.05
S2823P	12.98	1.02	18.25	0.46	13.0	16.90	0.58	24.72		0.55	0.25	1617		85	21.5	7.44	8.82	8.08	0.04	0.23
S2851P	12.12	0.86	18.10	0.36	13.0	16.70	0.66	25.03		0.91	0.39	9303	9245	38	124.0	9.15	10.70	9.70	0.03	0.28
S2877N	13.19	1.21	18.43	0.54	10.4					1.12	0.56	2843		226	37.9	8.28	9.22		0.11	

Table 5a.1. Undetected objects – identifications and coordinates.

Number	2MASS hhmmss.s+ddmss (J2000.0)	PGC	others
S9O	0003379+202723	251	KUG 0001+201
S23P	0011013+212455	1649524	
S36O	0016316+161126	1088	CGCG 456–051
S39P	0017345+165932	1521966	
S43O	0019429+295607	1266	MCG +05-01-073
S46O	0020326+152050	1316	CGCG 434–002
S59P	0022507+144348	1465666	
S81O	0029264+172905	1803	MCG +03-02-014
S91P	0032551+151522	1479643	
L26O	0038478+142858	1459324	
L26O	0038478+142858	1459324	
S127P	0052560+154707	1493287	
S140P	0056468+300825	1891795	
S151P	0101437+270654	1798205	
S155P	0102205+325840	2019367	
S161P	0104249+211110	1644665	
S170P	0108172+320523	1979705	
S178P	0109059+144521	1466339	
S231P	0127383+331015	2025379	
S232N	0127498+335256		
S255P	0134529+265648	1793228	
S265P	0138385+184014	1566633	
S277P	0144058+251544	1730587	
S281P	0145233+173903	1538003	
S285P	0146569+323024	2000119	
S297P	0151172+232530	1687132	
S298P	0151249+223539	212849	
S304P	0155058+350930	2060317	
S305N	0155246+293208		
L81O	0155396+370219	7189	CGCG 522–068
S321P	0202002+202546	1627043	
S334P	0206477+153308	1487658	
S339N	0209081+355129		
S353N	0214024+120347		
S363N	0218220+243343		
S363N	0218220+243343		
S367P	0219203+371329	2095670	
S371P	0219285+344638	2054374	
S373P	0221246+291221	1858979	
S374O	0221511+172741		NPM1G +17.0095
S375P	0221555+370429	2092488	
S391N	0227189+210523		
S392P	0227455+152616	1484626	
S401P	0232496+230820	1682146	
S408P	0234434+373626	2104891	
L127N	0235567+322439		
S418P	0240025+174100	1538874	
S420N	0240466+201104		
S427P	0243239+330042	2020570	
S442P	0247409+353952	2068054	
S449P	0251314+125629	1419356	
S456P	0254471+220418	1662967	
S467P	0258283+250313	1724074	
S470P	0259404+233100	1688741	
S475P	0303350+354438	0138596	
S476P	0303350+355730	2072652	
S493P	0309074+233902	1691142	
S507P	0311112+202114	1624788	
S508P	0311147+210223	1641398	
S511P	0311462+244837	1717065	
S515P	0311568+201712	1622716	
S520N	0313382+293751		
S528P	0316152+364746	2087153	
S538P	0320409+342131	2047947	
S555P	0325481+352504	2064213	
S566P	0328112+355443	2071937	

Table 5a.2. continued.

Number	2MASS hhmmss.s+ddmss (J2000.0)	PGC	others
S578N	0333114+372306		
S579N	0333218+363754		
S584P	0334189+133015	1432686	
S592P	0337054+262739	1777125	
S595N	0338017+352013		
S606N	0339586+370010		
S617N	0346139+223529		
S625P	0349496+143540	1462056	
S627N	0350107+345319		
S645P	0358036+124505	1415508	
S647N	0358052+123215		
S648P	0358066+143907	1463532	
S651P	0358443+281647	1831323	
S656P	0402225+160138	1498974	
S657P	0402296+163915	1513823	
S678N	0412312+371943		
S682P	0413159+232625	1687428	
S685N	0413468+291419		
S695N	0418166+244733		
S712N	0423115+270553		
S713N	0423419+270952		
S719N	0424437+170356		
S720N	0424443+250341		
(S721N)	0424456+215937		
S732P	0427394+125244	1418001	
S741N	0432467+163006		
S748N	0437210+205834		
S752N	0439319+193411		
S755N	0440089+251236		
S776N	0446027+284054		
L253P	0447309+242207	1705745	
L254P	0448017+282610	1835693	
S781N	0448386+265821		
S833N	0503531+190758		
S866N	0520289+161402		
S968P	0640428+300108	1887003	
S977N	0652072+325615		
S989P	0656387+195403	1609491	
S991N	0658094+222151		
S992P	0658098+220545	1663418	
S997P	0704128+184613	1569747	
S999P	0704252+245205	1718701	
S1001P	0704363+261643	1770102	
S1002N	0705213+223658		
S1005P	0706340+204200	1633959	
S1009P	0708345+350120	2058199	
S1019O	0712255+234310	0200233	UGC 3737
S1024P	0715280+235241	1695360	
S1033P	0720185+234903	1694275	
S1036P	0722426+200807	1617572	
S1040P	0730350+181644	1555098	
S1045O	0734342+212549	1649818	NPM1G +21.0165
S1053O	0741001+125828	1420032	NPM1G +13.0153
S1063P	0747231+222040	1668196	
S1065O	0748160+183255	21842	CGCG 087–040
L325O	0749057+283709	21881	CGCG 148–034
S1073P	0752471+150449	1474712	
S1076P	0754330+230346	1680751	
S1078N	0755037+135034		
S1082P	0756012+214745	1657432	
S1087P	0759352+241455	1702995	
S1093P	0802276+305301	1922147	
S1095P	0802395+162202	1507084	

Table 5a.3. continued.

Number	2MASS hhmmss.s+ddmmss (J2000.0)	PGC	others
S1103P	0807110+154513	1492534	
S1104N	0807146+152700		
S1106N	0808130+162210		
S1107O	0808232+333322	79944	KUG 0805+337
S1122N	0816236+222258		
S1123P	0817159+245356	1719550	
S1126P	0818014+200941	1618445	
S1131P	0820233+352443	2064113	
S1132P	0820542+352929	2065321	
S1136P	0823238+193101	1595283	
S1152O	0828513+135937	1446299	NPM1G+14.0160
S1153P	0829166+174040	1538701	
S1159P	0832351+262617	1776283	
S1161P	0833064+211848	1647457	
S1163O	0834174+143251	24056	CGCG 089-048
S1164P	0834570+322655	1997387	
S1178P	0839382+253418	1741441	
S1189P	0846189+283336	1839359	
S1197P	0849521+265311	1791318	
S1208O	0856118+310754	25091	CGCG 150-046
S1209O	0856151+374520	86872	KUG 0853+379
S1212N	0856498+214950		
S1213P	0857172+201758	1623132	
S1217O	0857549+200713	25183	MCG +03-23-023
S1223N	0900332+161408		
S1227P	0902071+342936	2050068	
S1231P	0903115+272939	1809811	
S1238P	0905254+231056	1682899	
S1241O	0906584+175748	25576	CGCG 090-075
S1245P	0908571+213243	1652257	
L366N	0909504+205912		
S1258O	0914393+264158	26061	CGCG 151-033
S1276O	0920116+163149	26405	CGCG 091-072
S1290P	0925159+165633	1520768	
S1304O	0933170+343734	82426	KUG 0930+348
S1305O	0933543+340342	27171	KUG 0930+342
L370P	0915558+175541	1545556	
S1442P	1034434+202138	1624987	
S1446P	1036586+255441	1754829	
S1453O	1042375+183744	1565271	IRAS F10399+1853
S1472P	1052431+205946	1640487	
S1529P	1113409+200035	1613290	
S2477N	2008293+135344		
S2490N	2023589+185435		
S2506P	2046350+202947	1628981	
S2517N	2057454+121353		
S2518P	2057527+151552	1479876	
S2528P	2102030+272402	1806969	
S2529N	2102403+293515		
S2530N	2102454+293830		
S2531P	2102519+274722	1818059	
S2537N	2103472+310052		
S2539P	2105168+275416	1821098	
S2548P	2110483+305430	1923278	
S2562P	2120576+130851	1424009	
S2565P	2122429+291629	1861228	
S2566P	2124228+324224	2009018	
S2567P	2124430+323259	2002015	
S2568P	2125011+300315	1888382	
S2570P	2125182+324737	2012575	
S2571P	2128065+331359	2027067	
S2577N	2132406+130216		
L763O	2134186+331523	66980	CGCG 492-003
S2599P	2149069+232454	1686959	
S2600P	2149506+271425	1801987	
S2618O	2204537+355842	2073020	NPM1G+35.0445
S2623P	2206196+165931	1521961	
S2624P	2206284+331523	2027712	
L776P	2213271+371102	2094709	

Table 5a.4. continued.

Number	2MASS hhmmss.s+ddmmss (J2000.0)	PGC	others
S2633P	2214140+135232	1442967	
S2637P	2215114+155639	1497041	
S2647P	2217439+131913	1428111	
S2656N	2222133+325845		
S2657P	2222425+360630	2075096	
L784P	2223348+344727	2054604	
S2660P	2224312+310449		
S2668N	2229064+371958		
S2671P	2233178+173910	1538077	
S2675P	2236509+250947	1727399	
S2677O	2237175+194611	1604880	IRAS F22348+1930
S2684P	2239269+150126	1473220	
S2689P	2241018+251008	1727639	
S2693P	2242023+212644	1650151	
S2698P	2244193+172710	1533140	
S2699P	2244258+291907	1862570	
S2701O	2245344+315412	1970389	NPM1G +31.0474
S2718P	2251135+311448	1938378	
S2719O	2251143+312317	69868	MCG +05-53-022
S2725P	2253049+371110	2094761	
S2727P	2254200+321255	1986198	
S2729P	2255075+325256	2015903	
S2732N	2256491+161609		
L802P	2258027+322757	2800849	
S2738P	2301166+184415	1568687	
S2740N	2301349+190444		
S2742P	2302019+204907	1636581	
S2747P	2302342+122422	1408968	
S2749O	2303055+231818	85371	KUG 2300+230
S2750N	2303059+231501		
S2751P	2303160+204451	1635011	
S2779O	2312557+251404	85404	KUG 2310+249
S2789P	2316428+153954	1490363	
S2811O	2321082+121132	71163	KUG 2318+119
S2841P	2336272+211917	1647600	
S2842P	2336285+213113	1651697	
S2845P	2338309+232944	1688388	
S2875P	2351300+270316	1796457	
S2880P	2353019+251145	1728419	
S2891O	2357222+151252	73025	KUG 2354+149
S2892O	2357244+235258	85904	KUG 2354+236

No: source names in brackets are not found in later versions of the public 2MASS database.

Table 5b.1. Undetected objects – basic data.

No	K_{20} mag	$J - K$ mag	$H - K$ mag	μ_{K5} $\frac{\text{mag}}{r^2}$	b/a	r_{K20} ''	B_{Tc} mag	D_{25} '	$\mu_{B_{25}}$ $\frac{\text{mag}}{r^2}$	T	rms mJy	I_{HI} Jy km s ⁻¹	$\frac{M_{HI}}{L_K}$	$\frac{M_{HI}}{L_B}$	search mode
S9O	12.88	1.02	0.46	18.19	0.70	11.4	16.09	0.68	24.16	S	0.74	0.56	0.08	0.23	lo
S23P	13.15	0.81	0.31	18.44	0.57	10.2	16.30	0.62	24.25		1.52	1.14	0.21	0.57	lo
S36O	12.65	1.09	0.32	18.02	0.48	12.0	16.27	0.43	23.40		0.90	0.68	0.08	0.33	lo
S39P	13.67	1.66	0.93	18.70	0.40	10.2	18.00	0.30	24.45		0.94	0.71	0.21	1.70	lo
S43O	12.64	0.86	0.34	18.42	0.62	15.0	15.99	0.49	23.38		1.03	0.78	0.09	0.29	kv
S46O	12.83	1.08	0.39	18.54	0.78	12.0	15.19				1.01	0.76	0.10	0.14	lo
S59P	13.24	1.44	0.55	18.46	0.36	11.8	17.90	0.38	24.87		0.92	0.69	0.14	1.51	lo
S81O	13.65	1.14	0.54	19.30	0.56	11.0	17.30	0.35	24.20		1.52	1.14	0.34	1.44	lo
S91P	13.75	1.18	0.57	19.08	0.40	15.6	17.30	0.49	24.80		1.85	1.39	0.45	1.75	lo
L26O	12.51	1.05	0.41	18.48	0.29	24.4	16.00	0.78	24.64		1.28	0.96	0.10	0.37	lo
											1.10	0.82	0.08	0.31	hi
S127P	13.40	1.17	0.58	18.80	0.32	11.6	17.50	0.36	24.41		1.11	0.83	0.19	1.26	lo
S140P	13.03	1.24	0.43	18.44	0.32	14.0	17.30	0.56	25.16		1.31	0.98	0.16	1.23	lo
S151P	13.60	1.23	0.53	18.74	0.34	11.2	17.40	0.47	24.85		1.22	0.92	0.26	1.27	lo
S155P	13.19	1.05	0.33	18.45	0.40	12.0	16.60	0.55	24.36		1.16	0.87	0.17	0.58	lo
S161P	13.36	0.88	0.17	18.46	0.48	10.2	16.90	0.51	24.39		0.74	0.56	0.13	0.49	lo
S170P	12.43	0.98	0.20	18.02	0.60	14.2	15.80	0.52	23.45		0.98	0.73	0.07	0.23	kv
S178P	12.98	1.07	0.37	18.29	0.68	10.6	16.50	0.56	24.28		0.90	0.68	0.11	0.41	lo
S231P	12.76	1.03	0.19	18.30	0.32	15.4	16.50	0.74	24.86		1.18	0.88	0.11	0.53	lo
											1.97	1.48	0.19	0.89	hi
S232N	13.18	1.39	0.75	18.82	0.68	12.6					1.38	1.03	0.20		lo
											1.11	0.83	0.16		hi
S255P	12.77	1.06	0.33	18.13	0.68	11.8	16.70	0.39	23.87		0.88	0.66	0.09	0.48	lo
S265P	12.89	1.19	0.32	18.08	0.30	10.8	17.20	0.55	25.06		0.93	0.70	0.10	0.80	lo
S277P	13.35	1.13	0.42	18.50	0.33	10.2	16.90	0.59	25.10		1.25	0.94	0.21	0.82	lo
S281P	13.38	1.37	0.55	18.60	0.58	12.0	18.10	0.35	24.87		1.53	1.15	0.26	3.03	lo
S285P	13.65	1.02	0.30	18.87	0.30	10.4	17.40	0.48	24.78		1.08	0.81	0.24	1.12	lo
											2.25	1.68	0.49	2.32	hi
S297P	13.54	1.16	0.28	18.75	0.40	10.2	17.40	0.38	24.56		0.92	0.69	0.18	0.95	lo
S298P	13.32	0.85	0.27	18.47	0.56	11.2	16.70	0.42	23.85		1.12	0.84	0.18	0.61	lo
S304P	13.09	1.21	0.52	18.36	0.42	11.6	17.10	0.41	24.18		1.91	1.43	0.25	1.50	lo
S305N	13.11	1.12	0.56	18.39	0.62	10.4					0.98	0.73	0.13		lo
L81O	11.83	0.91	0.19	18.05	0.34	23.6	14.66	0.83	23.27	Sa	1.66	1.24	0.07	0.14	kv
S321P	13.31	1.49	0.58	18.47	0.50	10.2	17.70	0.30	24.33		0.93	0.70	0.15	1.27	lo
S334P	13.69	1.22	0.35	18.92	0.42	11.4	17.20	0.45	24.48		0.90	0.68	0.21	0.78	lo
S339N	13.50	1.37	0.58	18.57	0.32	10.8					1.67	1.25	0.32		lo
S353N	13.72	1.22	0.58	19.00	0.60	15.0					1.03	0.78	0.24		lo
											1.64	1.23	0.39		hi
S363N	12.94	1.10	0.35	18.23	0.42	10.7					0.90	0.68	0.10		lo
											1.29	0.97	0.15		hi
S367P	13.64	1.01	0.41	18.99	0.44	11.4	16.00	0.51	23.52		1.57	1.18	0.34	0.45	lo
											1.80	1.35	0.39	0.51	hi
S371P	13.57	0.94	0.19	18.70	0.40	10.2	17.00	0.38			1.32	0.99	0.27	0.95	lo
S373P	13.31	1.11	0.31	18.73	0.53	12.0	16.90	0.28	23.39		0.92	0.69	0.15	0.60	lo
											1.22	0.92	0.20	0.80	hi
S374O	13.16	1.02	0.51	18.51	0.62	10.2					0.96	0.72	0.13		lo
S375P	13.57	1.10	0.16	18.72	0.36	10.8	17.60	0.46	24.87		1.31	0.98	0.27	1.63	lo
											1.52	1.14	0.31	1.89	hi
S391N	12.95	1.25	0.39	18.30	0.42	12.0					1.06	0.79	0.12		lo
S392P	13.16	1.46	0.58	18.53	0.38	12.4	17.00	0.46	25.11		0.89	0.67	0.13	0.64	lo
S401P	12.72	1.11	0.16	18.44	0.66	16.6	15.80	0.51	23.95		0.88	0.66	0.08	0.21	lo
											0.87	0.65	0.08	0.21	hi
S408P	13.34	1.03	0.69	18.85	0.58	11.8	17.00	0.30	23.35		1.89	1.42	0.31	1.35	lo
L127N	12.35	1.01	0.40	18.21	0.38	22.0					1.16	0.87	0.08		lo
											1.24	0.93	0.08		hi
S418P	13.04	1.42	0.69	18.14	0.64	10.2	17.00	0.38	24.07		0.82	0.62	0.10	0.59	lo
S420N	12.78	1.36	0.73	18.15	0.42	13.0					1.45	1.08	0.14		lo
S427P	13.13	1.25	0.30	18.43	0.70	11.2	17.10	0.43	24.57		1.44	1.08	0.20	1.13	lo
S442P	12.90	1.35	0.57	18.15	0.30	11.2	17.20	0.52	24.97		1.47	1.10	0.16	1.26	lo

Table 5b.2. continued.

No	K_{20} mag	$J - K$ mag	$H - K$ mag	μ_{K5} $\frac{\text{mag}}{r^2}$	b/a	r_{K20} "	B_{Tc} mag	D_{25} '	μ_{B25} $\frac{\text{mag}}{r^2}$	T	rms mJy	I_{HI} Jy km s ⁻¹	$\frac{M_{\text{HI}}}{L_K}$	$\frac{M_{\text{HI}}}{L_B}$	search mode
S449P	13.11	1.40	0.85	18.48	0.46	12.0	16.70	0.37	24.11		1.72	1.29	0.23	0.93	lo
											0.94	0.71	0.13	0.51	hi
S456P	13.67	1.42	0.63	18.72	0.38	10.7	17.00	0.34	24.99		0.74	0.56	0.17	0.54	lo
S467P	13.45	1.15	0.36	18.55	0.40	11.0	17.20	0.44	24.67		0.89	0.67	0.16	0.77	lo
S470P	12.97	1.45	0.48	18.13	0.40	10.4	17.30	0.35	24.88		0.64	0.48	0.08	0.60	lo
S475P	12.89	1.11	0.32	18.13	0.48	10.2	16.40	0.41	24.60		1.21	0.91	0.13	0.50	lo
S476P	13.42	1.51	0.67	18.58	0.44	10.8	17.20	0.36	24.87		1.42	1.07	0.25	1.23	lo
S493P	13.66	1.09	0.42	18.79	0.52	10.8	17.40	0.30	24.41		0.81	0.61	0.18	0.84	lo
S507P	13.32	1.35	0.56	18.61	0.34	12.4	17.70	0.27	24.71		0.91	0.68	0.15	1.24	lo
S508P	12.60	0.98	0.24	18.03	0.58	12.8	15.70	0.56	24.15		0.92	0.69	0.08	0.20	lo
S511P	13.33	1.22	0.51	18.49	0.32	11.4	17.60	0.35	24.81		0.82	0.62	0.14	1.03	lo
S515P	12.97	1.40	0.56	18.24	0.46	10.4	16.80	0.43	24.88		1.14	0.86	0.14	0.68	lo
S520N	13.12	1.03	0.24	18.62	0.30	12.6					0.82	0.62	0.11		lo
S528P	12.97	1.13	0.32	18.32	0.73	11.2	15.80	0.42	23.88		1.40	1.05	0.16	0.33	lo
S538P	13.28	1.22	0.42	18.48	0.48	11.4	17.20	0.39	24.71		1.23	0.93	0.19	1.07	lo
S555P	12.87	1.12	0.39	18.03	0.54	10.2	16.60	0.31	23.92		1.25	0.94	0.13	0.62	lo
S566P	13.50	1.31	0.30	18.80	0.34	13.0	16.80	0.40	24.80		1.01	0.76	0.19	0.60	lo
											1.53	1.15	0.29	0.91	hi
S578N	13.04	1.60	0.68	18.26	0.44	11.0					1.47	1.10	0.18		lo
S579N	12.76	1.24	0.47	18.08	0.60	10.8					1.33	1.00	0.13		lo
S584P	13.02	1.24	0.53	18.62	0.70	11.0	15.90	0.40	24.62		0.91	0.68	0.11	0.24	lo
S592P	12.89	1.40	0.38	18.12	0.38	10.2	17.30	0.45	25.01		0.89	0.67	0.10	0.84	lo
S595N	13.12	1.12	0.42	18.36	0.64	10.2					1.30	0.97	0.17		lo
S606N	13.08	1.23	0.46	18.47	0.72	10.6					1.21	0.91	0.16		lo
S617N	12.94	1.44	0.74	18.21	0.90	10.2					0.91	0.68	0.10		lo
S625P	13.27	1.14	0.41	18.57	0.34	11.8	16.40	0.42	24.78		0.71	0.53	0.11	0.29	lo
S627N	13.57	0.97	0.30	18.90	0.41	11.2					1.31	0.98	0.27		lo
											1.15	0.86	0.23		hi
S645P	13.19	0.92	0.35	18.66	0.70	11.2	16.02	0.54	24.44		1.72	1.29	0.25	0.50	lo
S647N	13.42	1.40	0.77	18.74	0.38	11.4					0.90	0.68	0.16		lo
S648P	12.74	1.42	0.33	18.12	0.60	11.2	15.40	0.58	24.65		0.65	0.48	0.06	0.11	lo
S651P	12.69	1.09	0.31	18.48	0.71	14.8	16.40	0.45	24.31		0.88	0.66	0.08	0.36	lo
											1.01	0.76	0.09	0.42	hi
S656P	13.04	1.36	0.67	18.40	0.58	11.0	16.70	0.35	24.19		0.89	0.67	0.11	0.49	lo
											1.50	1.13	0.23	0.47	hi
S657P	12.73	1.20	0.35	18.03	0.32	12.0	15.80	0.59	25.27		0.84	0.63	0.08	0.20	lo
S678N	13.24	1.13	0.25	18.66	0.52	13.2					1.47	1.10	0.22		lo
S682P	12.60	1.35	0.50	18.13	0.34	15.6	16.00	0.50	24.52		0.83	0.63	0.07	0.24	lo
											1.07	0.80	0.09	0.30	hi
S685N	13.65	0.93	0.62	19.03	0.69	11.2					0.92	0.69	0.20		lo
											1.17	0.88	0.26		hi
S695N	13.25	1.61	0.83	18.43	0.46	11.0					0.83	0.63	0.13		lo
S712N	12.57	1.16	0.21	18.06	0.78	11.8					0.99	0.74	0.08		lo
S713N	13.51	1.35	0.74	18.63	0.40	10.6					0.94	0.71	0.18		lo
S719N	13.28	1.48	0.54	18.48	0.44	10.6					0.76	0.57	0.12		lo
S720N	12.77	1.65	0.62	18.08	0.64	10.6					0.98	0.73	0.10		lo
S721N	13.66	1.84	0.86	18.50	0.12	17.0					0.94	0.71	0.21		lo
											0.95	0.71	0.21		hi
S732P	13.19	1.41	0.47	18.31	0.32	10.4	16.90	0.34	25.30		0.87	0.65	0.13	0.57	lo
S741N	12.67	1.72	0.69	18.64	0.42	19.0					0.82	0.62	0.07		lo
S741N	12.67	1.72	0.69	18.64	0.42	19.0					0.97	0.72	0.09		lo
S748N	13.10	1.37	0.55	18.42	0.46	11.4					0.85	0.64	0.11		lo
S752N	12.88	1.25	0.43	18.28	0.30	13.8					0.91	0.68	0.10		lo
S755N	13.42	1.45	0.41	18.65	0.50	10.6					0.78	0.58	0.14		lo
S776N	13.12	1.31	0.23	18.74	0.22	15.0					0.88	0.66	0.12		lo
L253P	13.09	1.15	0.39	18.76	0.46	22.0	14.60	0.30	24.27		0.84	0.63	0.11	0.07	lo
L254P	12.65	1.07	0.36	18.40	0.33	22.4	15.40	0.33	24.49		1.10	0.82	0.10	0.18	lo
											0.96	0.72	0.08	0.16	hi
S781N	12.87	1.53	0.65	18.22	0.55	10.6					1.11	0.83	0.12		lo
S833N	12.81	1.41	0.54	18.19	0.56	11.8					1.00	0.75	0.10		lo
S866N	12.98	1.21	0.40	18.32	0.47	11.4					1.00	0.75	0.12		lo

Table 5b.3. continued.

No	K_{20} mag	$J - K$ mag	$H - K$ mag	μ_{K5} $\frac{\text{mag}}{r^2}$	b/a	r_{K20} "	B_{Tc} mag	D_{25} '	μ_{B25} $\frac{\text{mag}}{r^2}$	T	rms mJy	I_{HI} Jy km s ⁻¹	$\frac{M_{HI}}{L_K}$	$\frac{M_{HI}}{L_B}$	search mode
S866N	12.98	1.21	0.40	18.32	0.47	11.4					1.00	0.75	0.12		lo
S968P	12.71	1.43	0.52	18.01	0.36	13.8	17.00	0.68	25.59		0.87	0.65	0.08	0.62	lo
S977N	13.31	1.02	0.48	18.54	0.38	10.4					1.28	0.96	0.21		lo
S989P	12.99	1.23	0.31	18.29	0.38	12.4	17.10	0.42	24.28		0.76	0.57	0.09	0.60	lo
S991N	13.05	1.28	0.47	18.27	0.56	10.4					1.25	0.94	0.16		lo
S992P	13.04	1.20	0.61	18.32	0.66	11.6	17.70	0.30	24.21		0.89	0.67	0.11	1.22	lo
S997P	12.80	1.10	0.48	18.71	0.68	13.8	16.60	0.47	23.95		0.74	0.56	0.08	0.37	lo
											0.62	0.47	0.06	0.31	hi
S999P	13.20	1.43	0.52	18.37	0.36	10.2	18.10	0.41	25.23		0.82	0.62	0.12	1.63	lo
S1001P	13.08	1.48	0.67	18.39	0.44	11.8	17.60	0.34	24.25		0.81	0.61	0.11	1.01	lo
S1002N	13.51	1.18	0.60	18.69	0.42	10.6					1.05	0.78	0.20		lo
S1005P	12.87	1.26	0.52	18.14	0.35	12.4	17.30	0.32	23.96		0.83	0.63	0.09	0.79	lo
S1009P	13.19	1.24	0.64	18.44	0.52	11.0	17.10	0.40	24.21		1.16	0.87	0.17	0.91	lo
S1019O	12.97	1.10	0.42	18.27	0.60	10.8	17.40	0.35	24.16		1.02	0.77	0.12	1.06	lo
S1024P	12.84	1.30	0.53	18.05	0.60	11.4	17.30	0.30	23.73		0.86	0.64	0.09	0.81	lo
S1033P	12.70	1.36	0.83	18.14	0.74	11.0	16.70	0.50	24.26		0.77	0.57	0.07	0.41	lo
S1036P	12.67	1.09	0.27	18.05	0.54	11.4	16.00	0.69	24.34		0.74	0.56	0.07	0.21	lo
S1040P	14.10	1.01	0.43	19.01	0.62	11.8	17.10	0.33	23.69		1.04	0.78	0.35	0.82	lo
											1.00	0.75	0.33	0.79	hi
S1045O	12.78	1.13	0.46	18.02	0.58	10.8	16.70	0.40	23.70		0.88	0.66	0.09	0.48	lo
											1.03	0.78	0.10	0.57	hi
S1053O	12.56	1.12	0.51	18.03	0.80	12.8	16.40	0.41	23.48		0.84	0.63	0.07	0.35	lo
S1063P	12.84	1.07	0.49	18.25	0.84	10.6	16.50	0.40	23.53		0.83	0.63	0.09	0.38	lo
S1065O	13.28	1.05	0.48	18.42	0.48	12.0					0.71	0.53	0.11		lo
											0.89	0.67	0.14		hi
L325O	11.73	0.95	0.32	18.13	0.82	20.8	15.20	0.79	23.66		0.95	0.71	0.04	0.13	lo
S1073P	13.07	1.23	0.65	18.60	0.65	11.0	17.40	0.38	24.18		0.89	0.67	0.12	0.93	lo
S1076P	13.60	1.19	0.52	18.78	0.42	11.4	17.30	0.37	24.21		0.78	0.58	0.16	0.73	lo
S1078N	13.31	1.32	0.44	18.66	0.28	11.8					0.86	0.64	0.14		lo
S1082P	13.18	1.10	0.39	18.36	0.32	10.2	17.00	0.50	24.56		0.78	0.58	0.11	0.55	lo
S1087P	13.13	1.32	0.50	18.28	0.46	10.2	17.20	0.40	24.22		0.85	0.64	0.12	0.74	lo
S1093P	12.91	1.28	0.60	18.27	0.40	11.8	16.90	0.51	24.47		0.94	0.71	0.11	0.62	lo
S1095P	13.39	1.13	0.35	18.80	0.36	13.4	16.80	0.59	24.56		0.86	0.64	0.15	0.51	lo
S1103P	12.88	1.32	0.67	18.09	0.50	10.4	17.10	0.43	24.11		0.87	0.65	0.09	0.68	lo
S1104N	12.71	1.07	0.29	18.02	0.63	10.8					0.82	0.62	0.08		lo
S1106N	12.43	0.91	0.35	18.17	0.84	14.4					0.93	0.70	0.07		lo
S1107O	13.38	1.29	0.53	18.95	0.62	10.4	16.51	0.58	24.22	S	1.08	0.81	0.19	0.49	lo
S1122N	12.63	1.58	0.61	18.02	0.32	13.8					0.76	0.57	0.07		lo
S1123P	13.98	0.80	0.15	19.38	0.50	10.4	17.20	0.40	24.20		0.82	0.62	0.25	0.71	lo
S1126P	13.13	1.32	0.40	18.25	0.36	10.6	17.00	0.42	24.12		0.77	0.57	0.10	0.54	lo
S1131P	12.67	1.21	0.54	18.08	0.54	11.6	16.20	0.59	24.17		1.08	0.81	0.10	0.37	lo
S1132P	12.86	1.10	0.38	18.31	0.26	14.6	16.90	0.78	25.42		1.13	0.85	0.12	0.74	lo
S1136P	12.69	1.01	0.41	18.01	0.74	10.4	16.60	0.50	24.12		0.70	0.53	0.06	0.35	lo
S1152O	12.70	1.19	0.36	18.06	0.58	10.2	16.64	0.48	24.00		0.81	0.61	0.07	0.40	kv
S1153P	13.05	1.19	0.39	18.38	0.46	12.2	16.90	0.50	24.34		0.88	0.66	0.11	0.58	lo
S1159P	12.78	1.07	0.39	18.46	0.82	12.2	16.50	0.48	23.82		0.80	0.60	0.08	0.36	lo
S1161P	13.26	1.27	0.40	18.59	0.52	11.0	17.80	0.40	24.81		0.80	0.60	0.12	1.20	lo
S1163O	12.89	1.10	0.32	18.38	0.30	14.6	16.30	0.56	24.03		1.04	0.78	0.11	0.39	lo
S1164P	12.85	1.17	0.45	18.22	0.30	12.6	17.00	0.56	24.74		0.98	0.73	0.10	0.70	lo
S1178P	13.43	1.00	0.34	18.65	0.38	10.4	17.10	0.36	23.89		1.12	0.84	0.20	0.88	kv
S1189P	12.80	1.08	0.41	18.11	0.44	10.2	16.60	0.56	24.37		0.89	0.67	0.09	0.44	lo
S1197P	13.11	1.46	0.61	18.33	0.44	11.2	17.80	0.40	24.78		0.83	0.63	0.11	1.26	lo
S1208O	13.69	0.83	0.26	18.84	0.86	13.0	16.55	0.44	23.62		0.91	0.68	0.21	0.43	kv
S1209O	13.06	1.26	0.55	18.45	0.60	11.8	16.52	0.39	23.34	S	1.66	1.24	0.21	0.76	lo
S1212N	12.96	1.18	0.41	18.73	0.78	12.2					0.87	0.65	0.10		lo
S1213P	13.48	1.18	0.24	18.85	0.34	12.2	16.70	0.58	24.43		0.96	0.72	0.18	0.52	lo
S1217O	12.61	1.03	0.31	18.06	0.72	11.0	15.90	0.45	23.00	(Sb)	0.74	0.56	0.06	0.19	lo
S1223N	13.31	1.01	0.37	18.43	0.78	12.0					0.88	0.66	0.14		lo
S1227P	13.44	1.09	0.38	18.88	0.32	13.6	17.00	0.54	24.56		1.07	0.80	0.19	0.76	lo
S1231P	13.50	1.33	0.74	18.83	0.58	10.6	18.20	0.31	24.58		0.84	0.63	0.16	1.82	lo
S1238P	12.74	1.01	0.42	18.19	0.50	11.8	16.20	0.54	23.78		0.86	0.64	0.08	0.29	lo

Table 5b.4. continued.

No	K_{20} mag	$J - K$ mag	$H - K$ mag	μ_{K5} $\frac{\text{mag}}{r^2}$	b/a	r_{K20} "	B_{Tc} mag	D_{25} '	μ_{B25} $\frac{\text{mag}}{r^2}$	T	rms mJy	I_{HI} Jy km s ⁻¹	$\frac{M_{\text{HI}}}{L_K}$	$\frac{M_{\text{HI}}}{L_B}$	search mode
S1241O	12.28	1.11	0.37	18.16	0.54	17.4	15.75	0.60	23.57		1.04	0.78	0.06	0.24	lo
S1245P	12.82	1.14	0.39	18.11	0.46	13.6	16.58	0.50	24.00		0.74	0.56	0.08	0.34	lo
L366N	12.86	1.17	0.52	18.46	0.18	20.8					0.76	0.57	0.08		lo
											0.81	0.61	0.09		hi
S1258O	12.90	0.90	0.39	18.23	0.60	12.0	16.20	0.39	23.10		1.43	1.07	0.16	0.49	lo
S1276O	12.91	1.12	0.60	18.58	0.72	11.4	16.21	0.51	23.62		1.13	0.85	0.13	0.39	lo
S1290P	12.81	1.17	0.33	18.25	0.32	15.8	16.50	0.63	24.42		0.93	0.70	0.09	0.42	lo
S1304O	12.88	0.95	0.31	18.37	0.55	11.2	16.24	0.51	23.58	S	1.25	0.94	0.14	0.45	lo
S1305O	12.53	0.97	0.32	18.01	0.44	14.4	15.33	0.91	23.87	S	2.56	1.92	0.20	0.39	lo
L370P	12.52	1.30	0.42	18.29	0.20	22.4	16.30	0.71	24.49		2.22	1.67	0.17	0.84	lo
											0.91	0.68	0.07	0.34	hi
S1442P	12.70	1.48	0.59	18.07	0.28	14.0	17.80	0.56	25.49		1.39	1.04	0.13	2.08	lo
											1.64	1.23	0.15	2.46	hi
S1446P	12.97	1.09	0.34	18.32	0.46	12.6	17.20	0.47	24.40		0.99	0.74	0.12	0.85	lo
S1453O	12.90	1.14	0.35	18.21	0.56	10.6	16.30	0.51	23.74		1.56	1.17	0.17	0.59	lo
S1472P	13.28	1.22	0.39	18.57	0.34	11.2	17.10	0.48	24.38		2.33	1.75	0.37	1.83	lo
S1529P	13.19	1.11	0.30	18.52	0.54	10.2	17.30	0.47	24.50		1.01	0.76	0.15	0.96	lo
S2477N	12.76	1.38	0.54	18.14	0.46	13.4					1.46	1.09	0.14		lo
S2490N	12.72	1.24	0.55	18.17	0.64	11.2					0.97	0.72	0.09		lo
S2506P	13.63	1.47	0.52	18.88	0.42	10.2	18.00	0.32	24.86		0.84	0.63	0.18	1.51	lo
S2517N	13.02	1.55	0.81	18.72	0.57	12.0					0.81	0.61	0.10		lo
S2518P	13.96	1.32	0.36	18.95	0.33	10.4	17.80	0.32	24.60		0.70	0.53	0.21	1.06	lo
S2528P	12.80	1.43	0.79	18.27	0.36	12.4	16.20	0.50	24.75		0.98	0.73	0.10	0.33	lo
S2529N	13.06	1.37	0.40	18.16	0.44	10.4					0.97	0.72	0.12		lo
S2530N	12.86	1.30	0.52	18.15	0.36	13.0					0.96	0.72	0.10		lo
S2531P	12.42	1.06	0.32	18.24	0.58	15.4	15.50	0.50	23.85		0.91	0.68	0.06	0.16	lo
S2537N	12.87	1.22	0.44	18.06	0.44	10.2					0.98	0.73	0.10		lo
S2539P	12.76	1.37	0.62	18.37	0.48	14.0	16.30	0.36	23.60		0.91	0.68	0.09	0.34	lo
S2548P	13.71	1.23	0.52	18.94	0.37	10.4	18.30	0.35	25.59		0.93	0.70	0.22	2.21	lo
											0.98	0.73	0.23	2.31	hi
S2562P	13.30	1.01	0.35	18.49	0.46	10.4	17.10	0.32	23.74		0.81	0.61	0.13	0.64	lo
S2565P	13.12	1.36	0.40	18.50	0.37	11.4	17.10	0.51	25.19		0.87	0.65	0.12	0.68	lo
S2566P	12.87	1.27	0.39	18.18	0.43	12.0	16.20	0.45	24.16		1.07	0.80	0.11	0.37	lo
S2567P	13.37	1.16	0.37	18.72	0.46	11.2	16.80	0.44	24.78		0.93	0.70	0.16	0.56	lo
S2568P	13.25	1.28	0.42	18.57	0.54	11.0	16.90	0.38	24.37		1.01	0.76	0.15	0.66	lo
S2570P	13.62	1.13	0.39	18.84	0.36	10.8	17.40	0.38	24.93		1.11	0.83	0.24	1.15	lo
S2571P	13.24	1.30	0.66	18.89	0.68	12.0	16.40	0.69	25.17		1.00	0.75	0.15	0.41	lo
S2577N	12.96	0.99	0.35	18.15	0.50	10.6					0.89	0.67	0.10		lo
L763O	11.84	0.98	0.25	18.16	0.31	26.4	15.26	0.76	24.12		1.11	0.83	0.05	0.16	lo
S2599P	13.15	1.08	0.27	18.43	0.44	10.2	16.60	0.65	24.81		0.84	0.63	0.12	0.42	lo
S2600P	12.91	1.47	0.41	18.23	0.36	12.0	16.80	0.54	24.54		0.90	0.68	0.10	0.54	lo
S2618O	12.90	1.05	0.57	18.30	0.72	10.8	16.40	0.35	23.62		1.15	0.86	0.13	0.47	lo
											1.31	0.98	0.14	0.54	hi
S2623P	12.87	0.88	0.31	18.58	0.86	13.0	16.10	0.51	23.63		1.13	0.85	0.12	0.35	lo
S2624P	12.88	1.28	0.68	18.29	0.76	12.2	16.70	0.41	24.13		0.97	0.72	0.10	0.52	lo
											1.03	0.78	0.11	0.57	hi
L776P	11.69	0.93	0.17	18.15	0.72	23.0	15.20	0.85	24.31		1.40	1.05	0.05	0.19	lo
											1.65	1.24	0.06	0.23	hi
S2633P	12.90	0.76	0.07	18.21	0.84	10.4	16.30	0.41	23.40		1.22	0.92	0.14	0.46	kv
S2637P	12.67	1.00	0.25	18.20	0.48	14.4	15.80	0.60	23.70		1.03	0.78	0.09	0.25	lo
S2647P	12.48	1.23	0.49	18.13	0.56	15.6	16.10	0.51	23.78		1.02	0.77	0.08	0.32	kv
S2656N	13.68	1.41	0.77	18.69	0.38	10.2					1.04	0.78	0.24		lo
L784P	12.85	1.40	0.56	18.55	0.21	20.4	17.10	0.66	25.47		1.12	0.84	0.12	0.88	lo
S2657P	13.17	0.91	0.26	18.59	0.44	10.8	16.40	0.46	24.02		1.17	0.88	0.17	0.48	lo
S2660P	13.85	1.25	0.48	19.19	0.30	12.2	18.05	0.22	23.86		1.05	0.78	0.28	1.96	lo
S2668N	13.53	0.82	0.28	18.71	0.68	10.2					1.40	1.05	0.28		lo
S2671P	13.40	1.33	0.61	18.92	0.26	12.6	17.50	0.55	25.20		0.76	0.57	0.13	0.86	lo
S2675P	12.95	1.20	0.34	18.57	0.76	14.8	16.90	0.50	24.36		0.87	0.65	0.10	0.57	lo
S2677O	13.25	1.49	0.74	18.55	0.44	11.2	17.20	0.33	23.80		0.73	0.55	0.11	0.63	lo
S2684P	13.33	1.46	0.49	18.87	0.82	10.2	17.40	0.32	24.09		0.78	0.58	0.13	0.80	lo
S2689P	12.88	1.25	0.51	18.20	0.82	10.2	16.80	0.45	24.11		0.80	0.60	0.09	0.48	lo

Table 5b.5. continued.

No	K_{20} mag	$J - K$ mag	$H - K$ mag	μ_{K5} $\frac{\text{mag}}{\text{mag}^2}$	b/a	r_{K20} "	B_{rc} mag	D_{25} '	μ_{B25} $\frac{\text{mag}}{\text{mag}^2}$	T	rms mJy	I_{HI} Jy km s ⁻¹	$\frac{M_{\text{HI}}}{L_K}$	$\frac{M_{\text{HI}}}{L_B}$	search mode
S2693P	13.38	1.04	0.32	18.53	0.56	10.4	17.00	0.37	23.87		0.86	0.64	0.15	0.61	lo
S2698P	13.15	1.35	0.75	18.41	0.40	11.4	17.60	0.42	24.74		0.71	0.53	0.10	0.88	lo
S2699P	12.67	1.09	0.67	18.18	0.72	10.4	16.20	0.47	23.63		0.86	0.64	0.08	0.29	lo
S2701O	12.88	1.13	0.38	18.12	0.54	11.0	16.31	0.52	24.00		1.33	1.00	0.14	0.50	lo
											1.20	0.90	0.13	0.45	hi
S2718P	12.48	1.03	0.34	18.11	0.60	14.0	15.80	0.68	24.08		0.95	0.71	0.07	0.22	lo
S2719O	13.38	0.76	0.17	18.97	0.66	14.2	15.80	0.51	23.51		1.10	0.82	0.19	0.26	lo
S2725P	13.24	1.44	0.63	18.51	0.40	11.6	17.30	0.39	24.59		1.28	0.96	0.19	1.21	lo
S2727P	13.16	1.42	0.40	18.45	0.26	12.2	17.70	0.48	25.18		0.95	0.71	0.13	1.29	lo
S2729P	13.29	0.95	0.10	18.70	0.64	15.4	15.90	0.56	23.88		0.97	0.72	0.15	0.25	lo
S2732N	12.83	1.25	0.65	18.17	0.72	10.6					0.98	0.73	0.10		lo
L802P	12.34	1.13	0.34	18.15	0.27	20.4	15.40				1.19	0.89	0.08	0.19	lo
S2738P	13.08	0.88	0.30	18.59	0.30	14.4	16.50	0.65	24.68		0.75	0.57	0.10	0.34	lo
S2740N	13.94	1.21	0.59	19.05	0.41	11.6					0.85	0.64	0.25		lo
S2742P	12.60	1.16	0.30	18.25	0.32	17.4	15.90	0.68	24.71		0.94	0.71	0.08	0.25	lo
S2747P	13.05	1.70	0.89	18.51	0.46	12.8	17.70	0.34	24.96		0.75	0.57	0.10	1.04	lo
S2749O	12.91	1.09	0.27	18.24	0.80	10.6	15.98	0.35	23.14	S	0.85	0.64	0.10	0.24	lo
S2750N	13.35	1.04	0.33	18.70	0.42	12.0					0.88	0.66	0.15		lo
S2751P	13.13	1.00	0.26	18.39	0.58	11.0	16.60	0.36	23.91		0.85	0.64	0.12	0.42	lo
S2779O	12.47	1.11	0.37	18.07	0.76	12.8	15.81	0.48	23.26	S	0.94	0.71	0.07	0.23	lo
S2789P	13.14	1.11	0.51	18.66	0.70	11.0	16.80	0.39	23.77		0.91	0.68	0.12	0.54	lo
S2811O	13.12	1.01	0.43	18.49	0.66	10.2	16.74	0.43	23.84	S	0.99	0.74	0.13	0.56	lo
S2841P	12.89	0.93	0.17	18.23	0.67	10.4	16.40	0.41	23.47		1.22	0.92	0.13	0.51	kv
S2842P	13.19	1.09	0.37	18.65	0.70	14.4	16.40	0.51	23.92		0.94	0.71	0.14	0.39	kv
S2845P	13.24	1.19	0.19	18.35	0.40	10.2	17.50	0.45	24.75		1.18	0.88	0.18	1.33	lo
S2875P	13.32	1.14	0.50	18.54	0.50	11.6	17.10	0.36	23.89		0.93	0.70	0.15	0.73	kv
S2880P	12.84	1.34	0.51	18.16	0.38	12.0	16.90	0.63	24.99		0.81	0.61	0.09	0.53	lo
S2891O	12.90	1.08	0.34	18.25	0.74	11.0	15.81	0.41	22.78	S	1.08	0.81	0.12	0.26	lo
S2892O	12.74	0.97	0.23	18.09	0.52	11.4	15.82	0.48	23.48		1.88	1.69	0.21	0.54	lo

Notes: 3 different H I line search modes were used: “lo” in the -500 to $11\,000$ km s⁻¹ range, “hi” in the 9500 to $21\,000$ km s⁻¹ range and “kv” for objects with previously known redshifts; Estimated upper limits to I_{HI} are for 250 km s⁻¹ wide, flat-topped profiles.

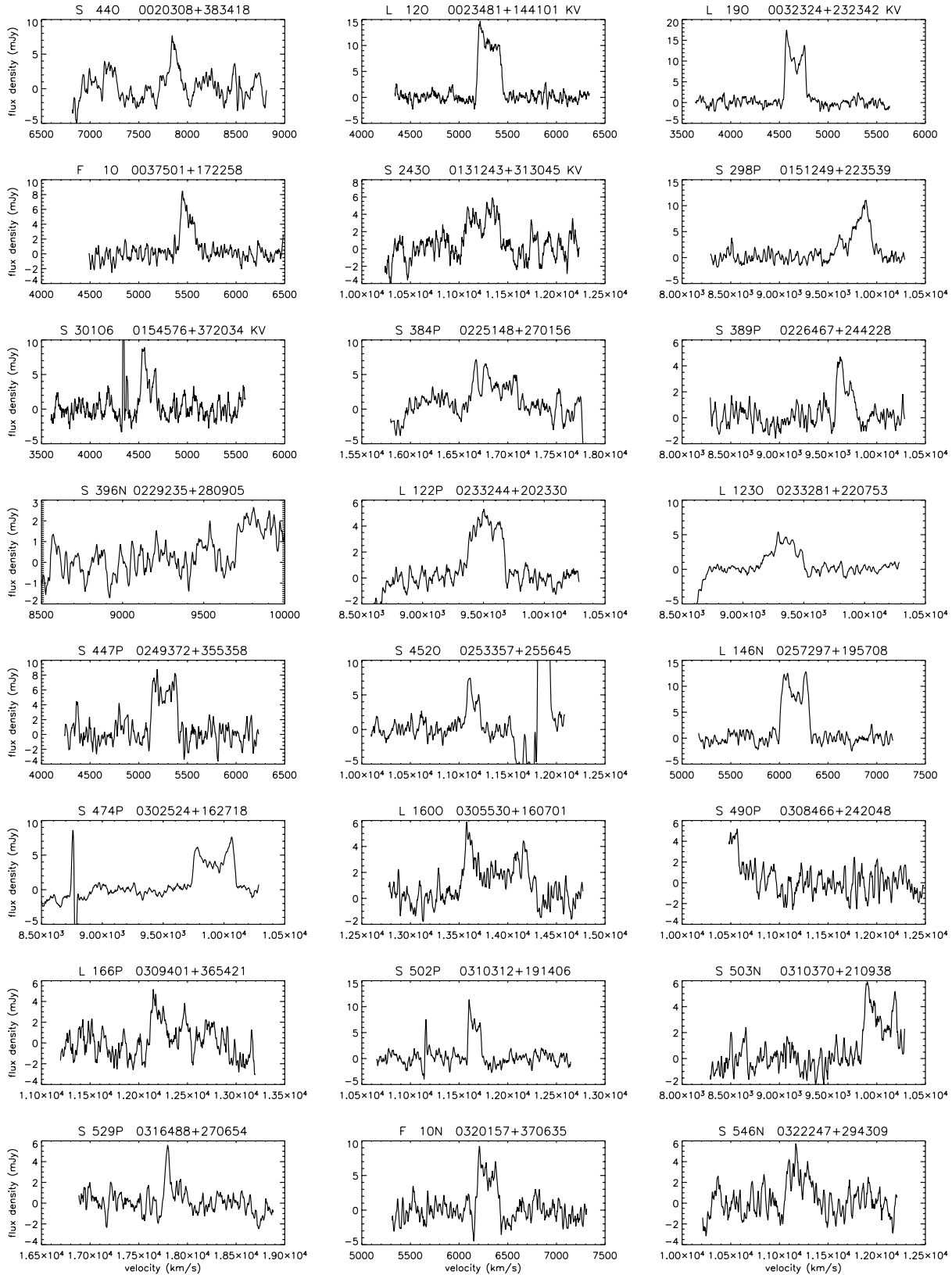


Fig. 2.a. Arecibo 21-cm H I line spectra of the clearly detected objects (see Table 3). Velocity resolution is 14.3 km s^{-1} (velocity search mode) and 16.4 km s^{-1} (known velocity mode), radial heliocentric velocities are according to the optical convention. Galaxies with previously known redshifts, detected in the “known velocity” mode, are indicated by the designation “KV” following their coordinates in the header of their spectrum.

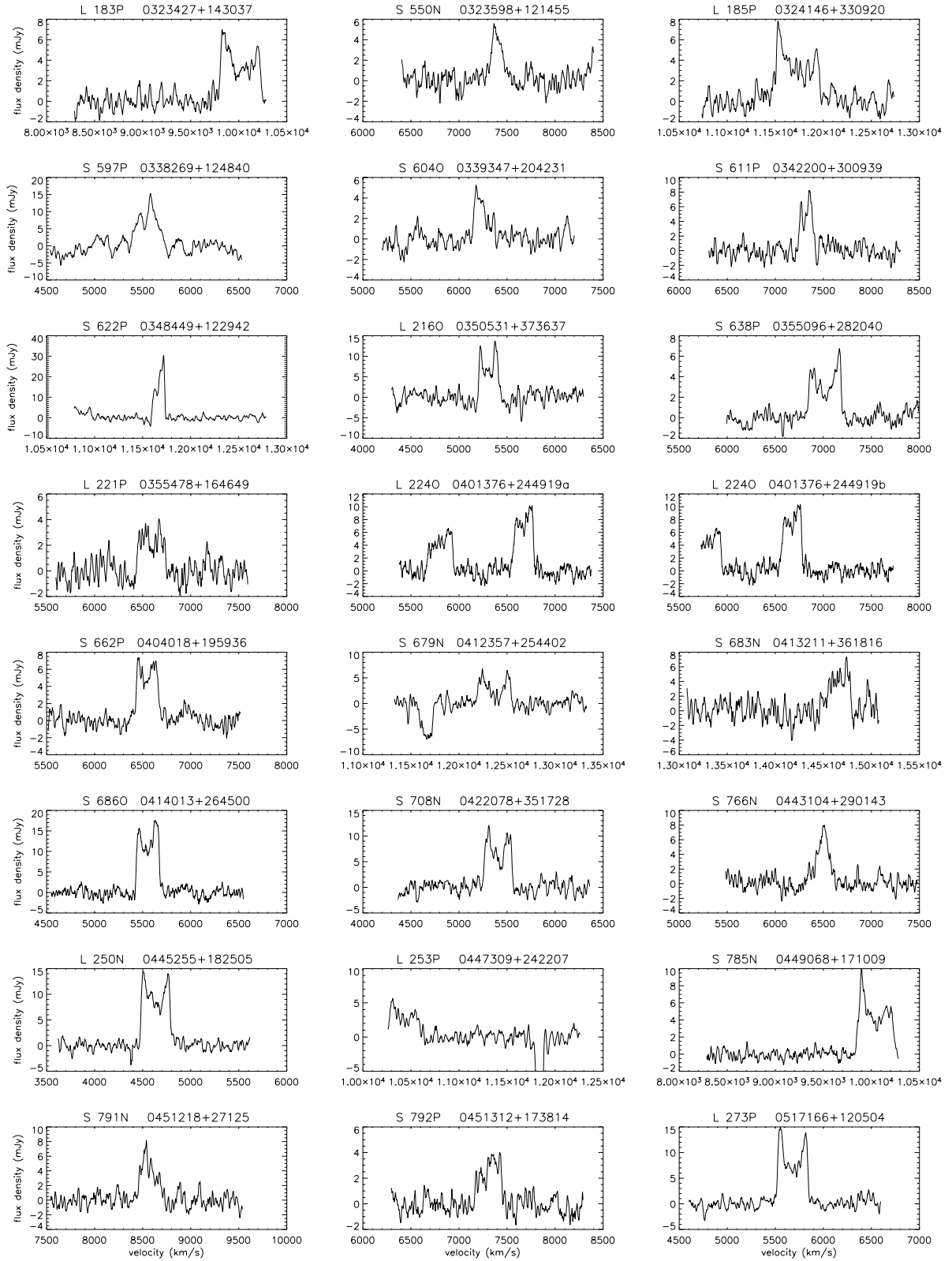


Fig. 2.b. continued.

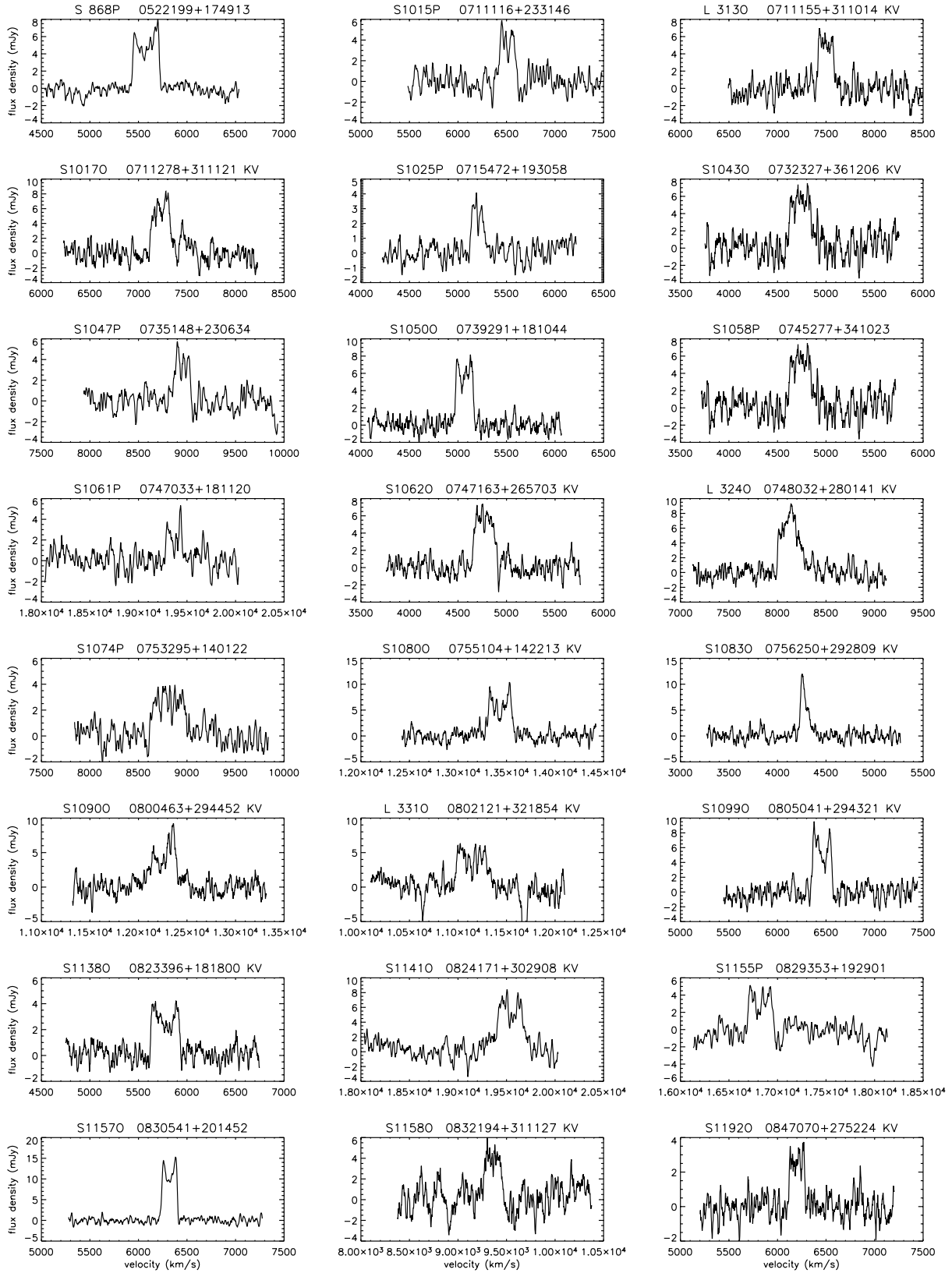


Fig. 2.c. continued.

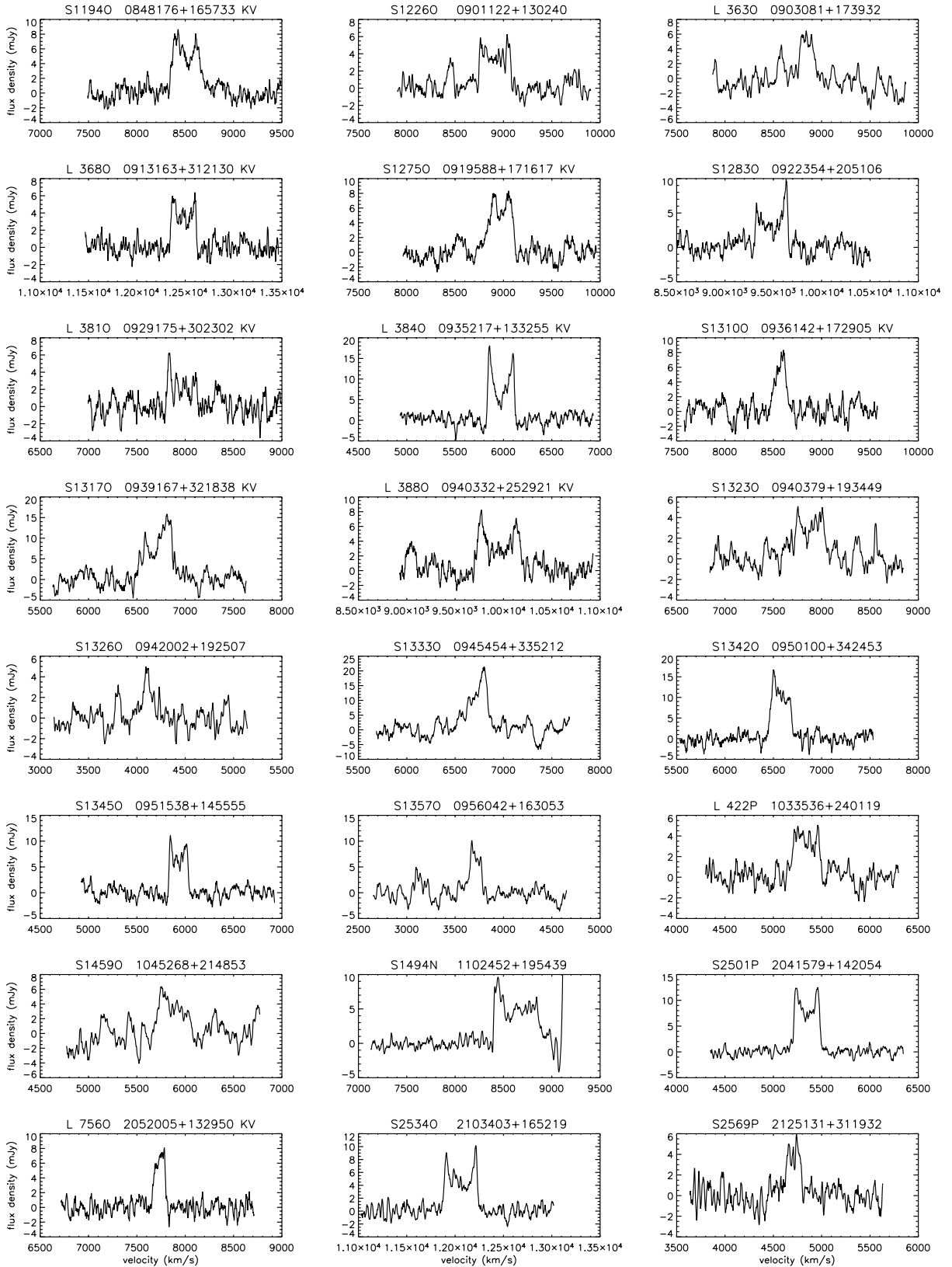


Fig. 2.d. continued.

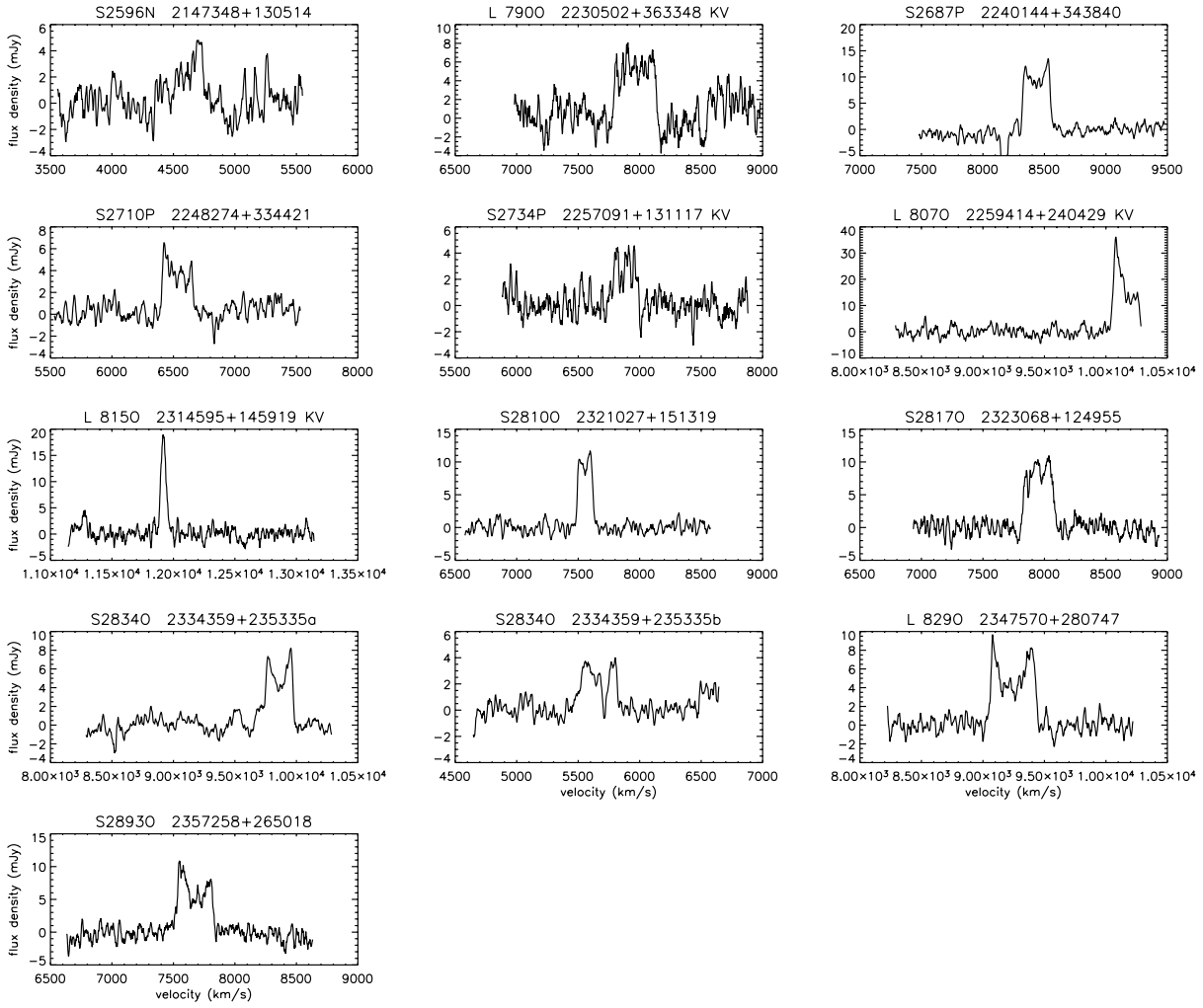


Fig. 2.e. continued.

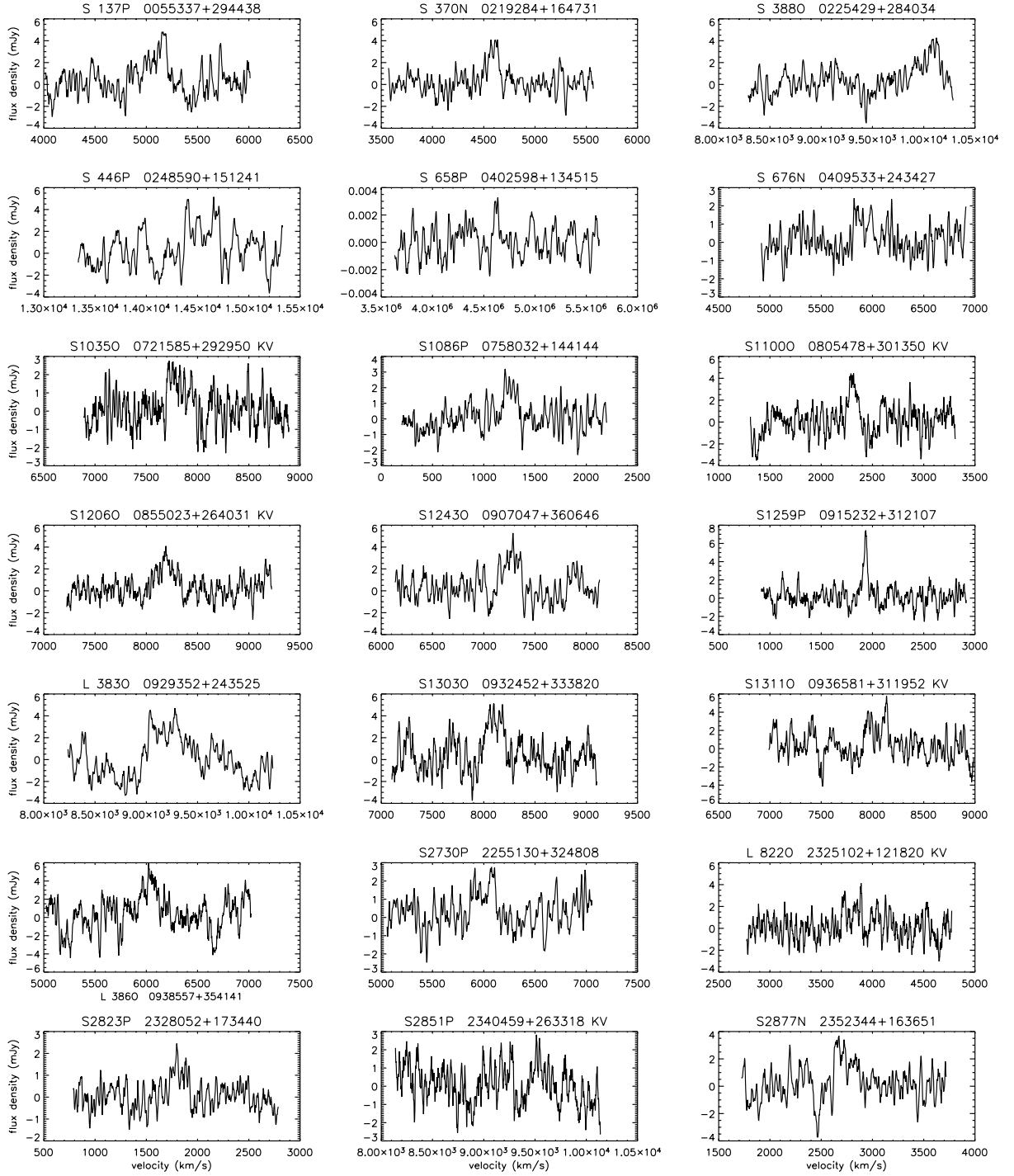


Fig. 3. Arcibo 21-cm HI line spectra of marginal detections (see Table 4). Velocity resolution is 14.3 km s^{-1} (velocity search mode) and 16.4 km s^{-1} (known velocity mode), radial heliocentric velocities are according to the optical convention. Galaxies with previously know redshifts, detected in the “known velocity” mode, are indicated by the designation “KV” following their coordinates in the header of their spectrum.